ADVANCES IN ENGINEERING TECHNOLOGY

VOLUME - 5

Chief Editor

Dr. Jaivir Singh
Associate Professor, Department of Engineering, SVPUAT Modipuram, Meerut, Uttar Pradesh, India

AkiNik Publications
New Delhi

Published By: AkiNik Publications

AkiNik Publications
169, C-11, Sector - 3,
Rohini, Delhi-110085, India
Toll Free (India) – 18001234070
Phone No. – 9711224068, 9911215212
Email – akinikbooks@gmail.com

Chief Editor: Dr. Jaivir Singh

Publication Year: 2021

Pages: 105

ISBN: 978-93-91538-43-9

Book DOI: https://doi.org/10.22271/ed.book.1410

Price: ₹ 715/-

Contents

Chapter - 1
Optical Coherence: Concepts and Applications

Author

Petro P. Trokhimchuck
Anatoliy Svidznskii, Department of the Theoretical and Computer Physics, Lesya Ukrayinka Volyn National University, Lutsk, Ukraine

Chapter - 1

Optical Coherence: Concepts and Applications

Petro P. Trokhimchuck

Abstract

Basic concepts of optical coherence are analyzed. Short historical analysis of this chapter of modern physics is represented. Main peculiarities of classic and quantum theory of optical coherence for free fields are discussed. Necessary of selection the light and structural parts of coherence in modern physics is proved. Main notions of coherent structures as third concept of Relaxed Optics are analyzed. The role of this concept in the development of modern optics, including Nonlinear Optics, holography and Relaxed Optics are discussed. Some applications this concept and its expansions are represented too.

Keywords: coherence, coherent structures, rayleigh ratio, quantum optics, holography, nonlinear optics, relaxed optics

I. Introduction

The problem of coherence (the name comes from the Latin word coherence-be in communication) is one of the central problems of modern optics and also of all modern physics [1-55]. This concept (ideal coherent and ideal noncoherent beams) is using for the explanation the interference and diffraction phenomena of electromagnetic waves). In first case, amplitudes of waves of optical fields sum up and superposition of light beams is observing as interference pattern. In second case intensities of optical fields and interference pattern isn't observing. In really, both cases are mathematical idealization because real optical beams are correlated mutually. Thus, the real light beams are partial coherent.

Theory of optical coherence for free electron fields is represented in [1-4].

In classical physics, coherence is called harmonization occurrence in space and time some oscillatory or wave processes [1, 5].

Quantum theory of coherence based on the theory of the quantum harmonic oscillator [1-4].

The analogy of classical and quantum coherence theory can be traced through N. Bohr modification of Rayleigh principle Heisenberg uncertainty principle [54].

The concept of the quantum harmonic oscillator can select the minimum difference between coherent and incoherent part of the modified Rayleigh principle as uncertainty principle. This difference (incoherent) above half the size and equal half of Planck's constant $\hbar/2$ [34].

In classical physics principle of coherence can be formulated based on the Rayleigh criterion [34, 54]:

$$\Delta k_x \Delta x = \Delta k_y \Delta y = \Delta k_z \Delta z = \Delta\omega\Delta t = 1. \quad (1)$$

Where $\Delta k_x, \Delta k_y, \Delta k_z, \Delta x, \Delta y, \Delta z, \Delta\omega, \Delta t$ – changes of the components of the wave vector, coordinates, frequency and time, respectively [54]. This criterion is used to separate spectral lines. Formally, the spatial part of the formula (1) can be used as a criterion for spatial coherence and temporal criterion of how temporal coherence. Strictly speaking for the separation of spectral lines in front of the unit should sign = can be replaced by a more or less $(\geq)$, and for coherence on a sign of lower – equal $(\leq)$. These relations for coherence may be written in the following form:

$$\Delta k_x \Delta x \leq 1, \quad \Delta k_y \Delta y \leq 1, \quad \Delta k_z \Delta z \leq 1, \quad (1a)$$

$$\Delta\omega\Delta t \leq 1. \quad (1b)$$

Formula (1a) is a principal of spatial coherence and (1b)-temporal coherence [1, 31-36].

The basic principle of quantum mechanics (uncertainty principle) and the main principle of coherence of quantum theory (quantum optics can formally get with help the ratio (1) multiplying it by the Planck constant, according N. Bohr [54]. They look like

$$\Delta p_x \Delta x = \Delta p_y \Delta y = \Delta p_z \Delta z = \Delta E\Delta t \leq \hbar. \quad (2a)$$

$$\Delta p_x \Delta x = \Delta p_y \Delta y = \Delta p_z \Delta z = \Delta E\Delta t \geq \hbar. \quad (2b)$$

Where $\Delta p_x, \Delta p_y, \Delta p_z, \Delta E$ – changes of proper components of linear momentum and energy. Equation (2a) can be represented as a principle of coherence of quantum theory and (2b)-the uncertainty principle.

In the experiment spatial and temporal coherence can't be selected in pure form [1-5, 34]. Because in classical optics used the difference between spatial and temporal coherence (phase coherence) $\varphi = \vec{k}\vec{r} - \omega t$.

But in real the coherence theory must be give answer on I. Newton phrase "The transitions of bodies into light and light into bodies obey the laws of nature, which, as it seems, amuses itself with these transformations" [47]. In whole, we must select the radiating (light) and structural (bodies) coherence. Therefore, the concept of coherent structures was creating as third concept of Relaxed Optics [34]. Main peculiarities this concept arec represented and discussed.

Elements of structural and light coherence are characterized main phenomena of Nonlinear Optics, including Cherenkov radiation, and holography.

II. Classic and quantum theories of coherence

Oscillations are called coherent if the phase difference is constant (or changes in any law) over time and for them it is possible to determine the total amplitude oscillattions [1].

Harmonic vibrations can be represented in the next form:

$$V(t) = A\cos(\omega t + \varphi) \tag{3}$$

Where A-amplitude, ω-frequency and φ-phase are constant.

Adding two oscillations with a frequency ω and different amplitudes A_1, A_2 and different phases φ_1, φ_2 resulting oscillation is also the frequency ω. The amplitude of this oscillation

$$A_s = \sqrt{A_1^2 + A_2^2 + 2A_1A_2\cos(\varphi_1 - \varphi_2)} \tag{4}$$

May change from $A_1 + A_2$ to $A_1 - A_2$ depending on the phase difference $\varphi_1 - \varphi_2$.

To assess the coherence of oscillations introduced correlation function $R(\tau)$, where the τ time interval of phase change in interval $\varphi_1 - \varphi_2 < \pi$.

The total amplitude of two attached oscillations with one source is changed according in the time interval τ according next formula

$$A_s = \sqrt{A_1^2 + A_2^2 + 2A_1A_2R(\tau)\cos\overline{\omega}\tau}, \quad (5)$$

Where $\overline{\omega}$ average frequency oscillations.

Value τ with $R(\tau) = 0{,}5$ is called coherence time.

With the propagation of a plane electromagnetic wave in a homogeneous medium oscillation phase does not change over time τ_0. In this case the wave propagates at a distance $c\tau_0$, where the c мудщсшен of light in vacuum. This distance $l_{coh} = c\tau_0$ is called the coherence length [1-11].

The concept of coherence used to describe a autooscillations with constant amplitude [1, 34] describe the properties of coherent waves in the direction perpendicular to the direction of propagation wave concept length and space coherence are introduced. Coherence length can be determined using the correlation function $R_\perp(l)$, where l is the appropriate sizes. Correlation $R_\perp(l) = 0{,}5$ determines the size or radius of coherence. Space waves can be divided into regions with constant coherence. The volume of this area (volume coherence) is determined by the product of the coherence length of the square shape with a radius $R_\perp(l) = 0{,}5R_\perp(0)$. This volume also correspond one cell of phase space.

Quite important characteristic of field is degeneration parameter δ [1, 56], which is equal to the average number of photons that are in the same state of polarization within the scope of coherence, that is the average number of photons of the same polarization, that coherence crossing the coherence in the coherence time. If N_ν-the average number of photons emitted per unit area per unit time of the light source in a single frequency range and the unit solid angle of the axis, which coincides with the normal to the surface of source, then

$$\delta = \frac{1}{2} N_\nu S \Delta\nu \Delta\Omega \Delta t. \tag{6}$$

The factor ½ on the right side (6) occurs because of the nature of thermal light sources. Thus, the light isn't polarized, that is equally both orthogonal polarization. From (1 b) and (6) we get value

$$\delta \approx \frac{c^2}{2\nu^2} N_\nu, \tag{7}$$

Which is not depend from geometry. For radiation blackbody we have

$$N_\nu = \frac{2\nu^2}{c^2}\left[\exp\left(\frac{h\nu}{k_B T}\right) - 1\right]^{-1}, \tag{8}$$

Where k_B – Boltzmann constant, T – absolute temperature.

In this case (8) takes the form

$$\delta \approx \left[\exp\left(\frac{h\nu}{k_B T}\right) - 1\right]^{-1}. \tag{9}$$

This formula was first obtained by A. Einstein [56] in the study of radiation in the cavity at its thermal equilibrium with the walls. The value describes the average number of photons in the cell of phase space and it called parameter of degeneration radiation.

This option can be applied for non-thermal radiation. So for a laser radiation $\delta >> 1,$ and for heat radiation $\delta << 1.$

Volume coherence coincides with the quantum mechanical definition of a cell of phase space, that is $\Delta q_x \Delta q_y \Delta q_z = h^3 \left(\Delta p_x \Delta p_y \Delta p_z\right)^{-1} \equiv \Delta V,$ where q, p-canonical coordinates and momentums.

In general, the correlation function can not depend only on the spatial coordinates or time. In the experiment, these two cases can be realized. Michelson interferometer is an example of temporal coherence, while Young's interference-spatial coherence. From a mathematical point of view the correlation function can be written as [1]

$$R(r,t) = R_1(r) R_2(t). \tag{10}$$

The concept of coherence is used to describe the wave properties of electrons, neutrons and other particles. In this case directed orderly flows of particles are coherent.

We must introduce basic concepts of coherence theory according to [1].

Imagine optical signal. which was introduced by D. Gabor [42], has next form

$$V(t)=\frac{1}{2}\left[V^{r}(t)+iV^{i}(t)\right], \tag{11}$$

Where

$$V^{i}(t)=-2\int_{0}^{\infty}\left|\tilde{V}^{r}(\nu)\right|\sin\left[2\pi\nu t-\arg\tilde{V}^{r}(\nu)\right]d\nu. \tag{12}$$

Correlation function of (m + n) order is determined as ensemble average from product the quantities for various space-time points with various polarizations in the next form [1]

$$\Gamma^{(m,n)}_{\mu_1,\ldots,\mu_{m+n}}(\vec{x}_1,\ldots,\vec{x}_{m+n};t_1,\ldots,t_{1m+n})=\left\langle\prod_{j=1}^{m}V^{*}_{\mu_j}(\vec{x}_j,t_j)\prod_{k=m+1}^{m+n}V^{*}_{\mu_k}(\vec{x}_k,t_k)\right\rangle, \tag{13}$$

Where brackets $\langle\ \rangle$ is operation of full averaging [1].

Corresponding to (13) quantum correlation functions, which can be used for the representation coherent of properties of photodetection fields, may be written as

$$\Gamma^{(m,n)}_{\mathrm{N},\mu_1,\ldots,\mu_{m+n}}(x_1,\ldots,x_{m+n})=Sp\left\{\hat{\rho}\prod_{j=1}^{m}A^{(-)}_{\mu_j}(x_j)\prod_{k=m+1}^{m+n}A^{(+)}_{\mu_k}(x_k)\right\}. \tag{14}$$

Where $x=(\vec{x},t)$, $A^{(+)}_{\mu},A^{(-)}_{\mu}$ – photon production and annihilation operators, Sp – trace of matrix, index N show, that product operators $A^{(+)}_{\mu},A^{(-)}_{\mu}$ is normal.

Degree of coherence may be determined as [1]

$$\gamma^{(n,n)}(x_1,\ldots,x_{2n})=\frac{\Gamma^{(n,n)}(x_1,\ldots,x_{2n})}{\left\{\prod_{j=1}^{2n}\Gamma^{(1,1)}(x_j,x_j)\right\}^{1/2n}}, \tag{15}$$

$$ {}^{(G)}\gamma^{(n,n)}\left(x_1,...,x_{2n}\right)=\frac{\Gamma^{(n,n)}\left(x_1,...,x_{2n}\right)}{\left\{\prod_{j=1}^{2n}\Gamma^{(n,n)}\left(x_j,...,x_j\right)\right\}^{1/2}}, \tag{16} $$

$$ {}^{(s)}\gamma^{(n,n)}\left(x_1,...,x_{2n}\right)=\frac{\Gamma^{(n,n)}\left(x_1,...,x_{2n}\right)}{\left[\Gamma^{(n,n)}\left(x_1,...,x_n,x_n,...,x_1\right)\Gamma^{(n,n)}\left(x_{n+1},...,x_{2n},x_{2n},...,x_{n+1}\right)\right]^{1/2}}. \tag{17} $$

For the representation of polarized properties of light we can introduce coherence matrix. In further we will be use only electrical field $\vec{E}$. Let electromagnetic waves are propagating along positive direction of axis *z* in right-handed coordinate system (*x*, *y*, *z*). Imagine analytical signals of this wave are quantities $E_x\left(\vec{x},t\right)$ and $E_y\left(\vec{x},t\right)$ j – mutually perpendicular and perpendicular to axis z components, $E_z=0$ (condition of transverse wave) [1].

Coherence matrix is written in next form

$$ G\left(\tau\right)=\left\langle\begin{pmatrix}E_x^*\left(t\right)\\E_y^*\left(t\right)\end{pmatrix}\times\left(E_x\left(t+\tau\right),E_y\left(t+\tau\right)\right)\right\rangle, \tag{18} $$

Where × is sign of direct Kronecker product.

Spectral coherence matrix is determined as

$$ R\left(\nu\right)=\begin{pmatrix}R_{xx}\left(\nu\right) & R_{xy}\left(\nu\right)\\R_{yx}\left(\nu\right) & R_{yy}\left(\nu\right)\end{pmatrix}=\lim_{T\to\infty}\frac{1}{2T}\left\langle\begin{pmatrix}\tilde{E}_x^*\left(\nu\right)\\\tilde{E}_y^*\left(\nu\right)\end{pmatrix}\times\left(E_x\left(\nu\right),E_y\left(\nu\right)\right)\right\rangle. \tag{19} $$

Spectral coherence matrix is hermitian but coherence matrix is hermitian for $\tau=0$ only.

Matrix $R\left(\nu\right)$ may be written as

$$ R\left(\nu\right)=\frac{1}{2}\begin{pmatrix}s_0+s_1 & s_2+is_3\\s_2-is_3 & s_0-s_1\end{pmatrix}, \tag{20} $$

Where $s_0=R_{xx}+R_{yy}, s_1=R_{xx}-R_{yy}, s_3=R_{xy}+R_{yx}, s_4=R_{xy}-R_{yx}$ are spectral Stokes parameters.

$$SpR = R_{xx} + R_{yy} = s_0 = \tilde{I}(\nu), \tag{21}$$

Where $\tilde{I}(\nu)$ is spectral intensity.

Using Pauli matrixes σ_i we can write spectral coherence matrix in next form [1]

$$R = \frac{1}{2}\sum_{i=1}^{3} s_i \sigma_i. \tag{22}$$

Spectral Stokes parameters may be determined as

$$s_i = Sp(\sigma_i R) \tag{23}$$

Analogous results can receive for coherence matrix $G(0)$ for quasi-monochromatic light and $\tau << 1/\Delta\nu$. In this case Stokes parameters $S_j(0) = S_j$ are determined as

$$S_j(\tau) = \int_0^{\infty} s_j(\nu)\exp(-i2\pi\nu t)\,d\nu. \tag{24}$$

Problem of polarized and unpolarized light may be resolved with help coherence matrix in next way. Coherence matrix may be represented as sum of polarized and unpolarized terms [1]

$$G = G_p = G_u, \tag{25}$$

Where

$$G_u = \begin{pmatrix} A & 0 \\ 0 & A \end{pmatrix}, \quad G_p = \begin{pmatrix} B & D \\ D^* & C \end{pmatrix}. \tag{26}$$

A degree of polarization P is determined as

$$P = \frac{SpG_p}{SpG_p + SpG_u} = \frac{B+C}{B+C+2A} = \sqrt{1 - \frac{4\det G}{(SpG)^2}} = \left|\frac{A_1 - A_2}{A_1 + A_2}\right| = \frac{\sqrt{S_1^2 + S_2^2 + S_3^2}}{S_0}. \tag{27}$$

Next formula is true

$$0 \le P \le 1. \tag{28}$$

Stellar Hanbery Brown-Twiss interferometer (Fig. 1) is example of correlation interferometry of fourth order. It may be explained with help methods of classic and quantum coherence [1, 28, 34, 57]. It measures only the intensity fluctuations of radiation, which falls on the detector. This method is "differentiation" of Michelson method. It logs the focus is likely the product of two intensities, not one. Signal of quadratic detector [28, 34] is equaled

$$\left|E^{(+)}(r_1,t)\right|^2 = |A|^2 + |B|^2 + AB^* e^{i(k-k')r_1} + A^* B e^{-i(k-k')r_1}. \quad (29)$$

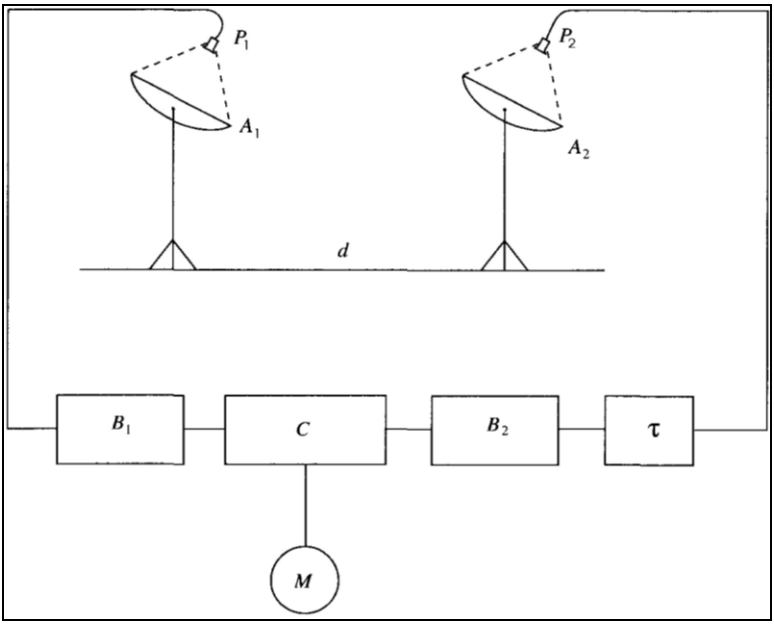

Fig 1: Schematic diagram of Hanbury Brown-Twiss stellar intensity interferometer. Here P_1 and P_2 are the photodetectors, A_1 and A_2 are the mirrors, B_1 and B_2 are the amplifiers, τ is the delay time, C is a multiplier and M is the integrator [28]

This signal does not include a quick oscillations of detected wave, but the main value of this transformed signal does not include the interference component (with $\langle AB^* \rangle = 0$). The Hanbery Brown-Twiss interferometer multiplies the two transformed signals and then measures their main statistical significance. The main value of this product can be represented in the form (30).

$$\left\langle \left|E^{(+)}\left(r_1,t\right)\right|^2 \left|E^{(+)}\left(r_2,t\right)\right|^2 \right\rangle = \left\langle \left(\left|A\right|^2+\left|B\right|^2\right)^2 \right\rangle + 2\left\langle \left|A\right|^2 \left|B\right|^2 \right\rangle \cos\left[\left(k-k'\right)\left(r_1-r_2\right)\right], \tag{31}$$

Where the following conditions are imposed:

$$\left\langle \left|A\right|^2 A^* B \right\rangle = 0, \quad \left\langle \left|B\right|^2 AB^* \right\rangle = 0 \text{, etc.} \tag{32}$$

Although interferograms are interpreted with a help of universal averaging but in this experiment the averaging over time is too. But averaging over time is more complex as a universal homogenization. For the time averaging in interferometry should be taken into account that the plane waves in general case can't be purely monochromatic. This allows you to put that amplitude A and B are stochastic functions of time $A(t)$ and $B(t)$ [28].

Main principles of Hanbury Brown-Twiss interferometer may be explain on the basis theory of correlation too [1].

For case of particular polarized light, we have next dispersion correlations for our two photodetectors (Fig. 1).

$$\left\langle \left(\Delta n\right)^2 \right\rangle = \left\langle n \right\rangle \left[1+\frac{1}{2}\left(1+P^2\right)\left\langle n \right\rangle \frac{\xi(T)}{T} \right], \tag{33a}$$

$$\left\langle \Delta n_1 \Delta n_2 \right\rangle = \frac{1}{2}\left(1+P^2\right)\left\langle n_1 \right\rangle \left\langle n_2 \right\rangle \left|\gamma_{12}\left(0\right)\right|^2 \frac{\xi(T)}{T}. \tag{33b}$$

Where $\xi(T)$ determine as

$$\xi(T) \approx \xi(\infty) = \int_{-\infty}^{+\infty} \left|\gamma\left(t\right)\right|^2 dt, \tag{34}$$

Which may be represented as one of possible determinations of coherent time τ_c.

But Hanbary Brown-Twiss experimental data are represented with help classic continuous signals of photodetectors-photocurrents but no number of photons. But for comparatively large photocurrents photon numbers, n_1 and n_2 are proportional to corresponding photocurrents $S_1(t)$ and $S_2(t)$ on detectors outputs and T is "resolution time" [1].

A correlation of photocurrents fluctuations may be written as [1]

$$\left\langle \Delta S_1 \Delta S_2 \right\rangle = \frac{1}{2}\left(1+P^2\right)\left\langle S_1 \right\rangle \left\langle S_2 \right\rangle \left|\gamma_{12}\left(0\right)\right|^2 \frac{\xi(T)}{T}. \tag{35a}$$

$$\left\langle \left(\Delta S\right)^2 \right\rangle = \left\langle \Delta S_1 \Delta S_2 \right\rangle_{x_1=x_2}. \tag{35b}$$

An equation (35 a) is equivalence to equation (33 b). Quantum term, which corresponded $\left\langle n \right\rangle$ in (33 a), is absented for photocurrents. This result is true for strong field approximation, second term in (33 a) is larger as first [1].

The role of coherence in quantum theory is more important than in classical. Phase in quantum mechanics is the main characteristic of the wave function, unitary (quantum canonical) transformation and scattering matrix. In general, the concept of coherence in quantum theory was initiated by L. de Broglie in his concept wave-corpuscular dualism (particle is standing wave) [34].

Modern quantum theory based on the E. Schrödinger (1927) idea of coherence and was developed by Robert Glauber [3] and E. Sudarshan [4]. Coherent states of the electromagnetic field is defined by the ratio of the vacuum state

$$\left|\alpha\right\rangle = \hat{D}\left(\alpha\right)\left|0\right\rangle, \tag{36}$$

Where $\hat{D}\left(\alpha\right) = \exp\left(\alpha\hat{a}^+ - \alpha^*\hat{a}\right)$-shift operator, $\hat{a}, \hat{a}^+$-operators destruction and birth of particles. Coherent state is eigenvector of operator of destruction (annihilation) $\hat{a}$ with eigenvalues α [1].

The phase of the wave function in quantum mechanics has a deeper physical meaning than in classical physics. It includes action, energy, momentum, angular momentum of corresponding physical interactions. Therefore, coherence is one of the most important concepts of quantum mechanics. Roughly speaking, wave function in the form of the exponential phase factor $\vec{p}\vec{r} - Ht$ is coherent function, where H-Hamiltonian of system. Therefore, coherence process or phenomenon associated with basic physical quantities: energy and momentum.

The wave function in quantum mechanics can form orthonormal basis. Therefore, we can represent each quantum state as a function of the coherent

states, in other words to make a schedule of coherent states. Representation of coherent states is more natural as Fock presentation. These two representations bound by the following formula [1]

$$\left|\alpha\right\rangle = e^{-|\alpha|^2/2} \sum_{n=0}^{\infty} \frac{\alpha^n}{\sqrt{n!}} \left|n\right\rangle, \tag{37}$$

Where $\left|\alpha\right\rangle$ – coherent state, $\left|n\right\rangle$ – Fock state.

Equation (1 a), (1 b) and (2 a) do not share a coherent and incoherent part of the interaction. Roughly speaking, it is a condition of interference of two waves. However, these relationships allow you to select only coherent or incoherent part of the interaction. This problem was solved in quantum coherence theory (quantum optics), which is based on the concept of the harmonic oscillator [1, 34]. The principle of uncertainty with regard to this takes the form

$$\Delta p_x \Delta x = \Delta p_y \Delta y = \Delta p_z \Delta z = \Delta E \Delta t \geq \hbar/2. \tag{38}$$

This is caused with minimal energy of harmonic oscillator $\hbar\omega/2$ (vacuum state). This energy corresponds to the energy of the incoherent electromagnetic field or the difference between the total energy and "coherent" part of the energy [1, 34]. Therefore, quantum coherence theory selects incoherent part of energy from the N. Bohr concept of the uncertainty principle.

Uncertainty principle may be represented in next form too [34]:

$$\sigma_q \sigma_p \geq \hbar^2/4, \tag{39}$$

According H.P. Robertson for randomized to random variables [34]

$$\sigma_A \sigma_B \geq \left|\left\langle\left[\hat{A}\hat{B}\right]\right\rangle\right|^2/4, \quad \sigma_C = \left\langle\left(\Delta\hat{C}\right)^2\right\rangle \equiv \left(\delta C\right)^2, \quad \Delta\hat{C} = \hat{C} - \left\langle C\right\rangle. \tag{40}$$

In the modern interpretation the formulas (40) correspond to uncorrelated states. In 1930 E. Schrödinger and H.P. Robertson [34] generalized (40) as follows

$$\sigma_A\sigma_B \geq \left|\left\langle\left[\hat{A}\hat{B}\right]\right\rangle\right|^2 \Big/ 4\left(1-r^2\right), \tag{41}$$

Where

$$r = \sigma_{AB} \Big/ \sqrt{\sigma_A\sigma_B} \tag{42}$$

Correlation coefficient of values A and B and $|r| \leq 1,$

$$\sigma_{AB} = \left\langle\{\Delta A, \Delta B\}\right\rangle \Big/ 2 \equiv \left\langle\left(\left(\left\langle\hat{A}\right\rangle - \langle A\rangle\right)\left(\hat{B} - \langle B\rangle\right)\right) + \left(\left(\hat{B} - \langle B\rangle\right)\left(\hat{A} - \langle A\rangle\right)\right)\right\rangle \Big/ 2 = \tag{43}$$
$$= \left(\left\langle\hat{A}\hat{B} + \hat{B}\hat{A}\right\rangle\right) \Big/ 2 - \langle A\rangle\langle B\rangle$$

-cross-correlation of values A and B, which corresponds to the average meaning of operator error $\Delta\hat{K} = \hat{K} - \left\langle K\right\rangle.$

Schrödinger: Robertson uncertainty principle (41) is a generalization of the Heisenberg–Robertson uncertainty principle (40) for the case of correlated states and coincides with the last at r=0 [34].

Schrödinger: Robertson uncertainty principle [324] was used to analyze the motion of a particle with coordinate $q(t)$ and momentum $p(t)$ in the field of harmonic oscillator $V\left(t\right) = Mq^2\left(t\right)\omega^2\left(t\right) \Big/ 2$. Process of decreasing the frequency of oscillations $\omega\left(t\right)$is caused by the increase of the correlation coefficient $r(t)$,

$$r\left(t\right) = \left\langle q\hat{p}_q + \hat{p}_q q\right\rangle \Big/ 2\delta q\delta p_q \tag{44}$$

And change uncertainty principle

$$\delta q\delta p_q \geq \hbar \Big/ 2\sqrt{1-r^2}, \tag{45}$$

Where $\delta q \equiv \sqrt{q^2}, \quad \delta p_q \equiv \sqrt{p_q^2}.$ Formally [34], change of the correlation coefficient of uncertainty principle can be represented by a

simple substitution $\hbar \to \hbar^* \equiv \hbar / \sqrt{1-r^2}$. For the absence of correlation $(r \to 0)$ value $\hbar^* \to \hbar,$ and the uncertainty principle receive classic Heisenberg form

$$\delta q \delta p_q \geq \hbar / 2. \tag{46}$$

For the receiving of correlated states of particle with $|r| \to 1$ a of dispersion of coordinate $\langle q^2 \rangle$, momentum $\langle p^2 \rangle$ and their product increases indefinitely. Practically case $|r| \to 1$ corresponds to the expansion of the wave packet. Formally, this concept is equivalent to the concept of symmetry breaking.

In nonlinear optics, phase matching conditions are conditions the coherence of interaction. In this case they have spatial (geometric) nature [34]. For example, to generate a second harmonic range of angles for the observe the effect are 10'-30' [12]. Another example is the generation of laser radiation. For solid laser angular range for stable resonator is ~10' for unstable resonators ~10"-20" [49]. For semiconductor lasers this value is more large [19]. For holography, we need to have more coherence length value, this value is determined coherence light source (usually a laser) [41, 42, 44-46].

Violation of coherence makes the failure of the relevant phenomena. It should be associated with the violation of symmetry. This is equivalent concepts.

For the interaction of light with matter we have to consider the interaction of two partners: light and matter. Symmetry and the nature of light, the matter and their interaction causes the generation of proper processes and phenomena [34].

III. Coherent structures

The problem of the creation the Coherent Structures (CS) in Relaxed Optics (RO) [31-36] is the one of the general problem of this chapter of modern physics. Coherent structures are called the new phases or states of the matter, it were created after laser irradiation. Practically it is the “traces” of the interaction laser irradiation and matter in matter. These structures may be classified as first-order and second-order structures. One has various energetic and time conditions of the creation and stability. The problem of

the classification and modeling of these structures may be resolved with help short-range, long-range action and mixed approximations of the interaction light and solid. Basic results of these classification and some results of modeling CS are discussed and analyzed.

Relaxed Optics is researched the processes of the irreversible interaction light and solid. In the system with variable order (dynamic system) we must introduced conception of coherent structures. This conception must include the irradiated, matter and irradiated–matter parts, including second-order relaxed processes. The real dynamic–structural processes may be have experimental realization in our time because the laser and measurable equipment are existed in some physical laboratory in the time range from $10^{-15} s$ to few years. The changes of the matter after irradiation may be have various phases (crystal, polycrystalline, amorphous, liquid, periodical phase and gas). These phases have various order and transition between here now practically unknown. Unit theory its transitions is absented too. Therefore, the creation the conception of coherent structures is one of the possible ways of the resolution of this problem.

The necessity of the introduction the conception of coherent structures CS in modern physics is caused of the development of Relaxed Optics [31-36]. This concept is appended coherence theory and may be represented as coherent approximation of chronological energy concept of Relaxed Optics [31-36].

The problem of the classification CS is caused the physical character of interaction light and solid in RO [31-36].

The first-order effects of interaction light and solid (the properties of changing light) are researched in physical optics, including holography and nonlinear optics [31-36]. The opposite effects of this interaction (trace irradiation in matter) are the subject of the research in the radiation physics of status solid and photochemistry.

But the irreversible interaction light and solid has some peculiarities, which can't explain with help of methods of the radiation physics of status solid, physical optics and photochemistry. Therefore RO were created [31-36].

One of the central problems of RO is the creation of CS [31-36]. The CS in irradiated matter must be having various natures.

The CS (coherent structures) are called the structures with next properties:

1) These structures have the some order and symmetry.

2) It may be source for the generation and transformation of radiation, including light, linear and nonlinear optics).
3) It may be source for the generation and transformation of irradiated matter, including amorphous and crystal materials, (the pure effects of RO).
4) It may be source for the generation and transformation of the radiation and irradiated matter, (holography, mixed phenomena of RO).
5) It may be formed with help coherent irradiation.

More detail classification coherent structure and relation to concrete physical phenomena and parts of modern optics are represented in Table 1.

Classification of Table 1 is very approximate and rough. It is corresponded to classification of basic optical phenomena with point of Relaxed Optics, which are represented in Table 1.

According to the time of the interaction and formation these structures may be classified as structures of first-order range and second-order range interaction (Table 2).

Table 1: CS in basic chapters of modern optics [34]

Linear Optics	Nonlinear Optics	Quantum and Coherent Optics	Relaxed Optics
Coherent structures are stable and use for the transformation optical irradiation. Basic phenomena: diffraction, interference and other.	Coherent structures are stable or unstable (dynamic) and use for the receiving: 1. Basic nonlinear effects, including laser irradiation, generation of harmonics, up-conversion and other; 2. Basic effects of parametric crystallo-optics, including electro-and magnetooptical phenomena.	Structures may be transform after absorption of coherent light: 1. Absorption on the metastable structures-quantum photochemistry (irreversible phenomenon). 2. Absorption on the stable structures-external and inner photo effects. 3. Absorption or scattering of two or more coherent waves-optical holography and the converse of wave front and other. Remarks. 1. In this case the transformations of optical irradiation are researched. 2. Structure may be coherent and incoherent.	Structures may be: 1. Stable-effects of laser implantation of crystal structures; 2. Metastable-effects of laser annealing of ion-implanted layers with $h\nu > E_g$ and other photochemical processes. 3. Unstable-effects of the creation short life-time objects, including exciton drops, quantum dots, evaporation and other. 4. Mixing case is the sum cases 1, 2 and 3. Here are mixing effects of RO. Remarks. 1. In this case the transformations of structures are researched. 2. The structural part of holography is case 2 in this column. 3. Coherent light may generate coherent structures on incoherent structures. 4. Case remarks 2 and 3 in this part optics aren't researched.

Remark to Table 1: The transformation of structure and straight methods of here investigation are researched in RO only.

The first-order range CS have quantum character and may be represented as photochemical or crystal photochemical processes. One of the interesting problems of these phenomena is the problem of the nonadiabatic scattering light on valent and impurities bonds. This problem in the classical physics of status solid is represented as adiabatic. In radiation physics of status solid this problem is neglected. In RO it is one of the interesting problems (the oriental effect and the creation donor layers in semiconductors [31-36]).

The second-order range CS have, as rule, the wave nature (thermochemical, including annealing, plasmic, electromagnetic hydrodynamic structures, interferometrical phenomena and other [34]).

Quantum CS may be classified as multiphotonic $(h\nu < E_g)$, including monophotonic $(h\nu \sim E_g)$ and fractured structures $(h\nu >> E_g)$; where $h\nu$-quantum energy, E_g-bandgap of irradiated materials. The experimental research in this part of physics is absented almost.

Table 2: First-order range and second–order range CS of RO [34]

First–order range CS	Second–order range CS
1. First-order quantum effects and here structures.	1. Second-order quantum effects and here structures:
1) Creation “dangling bonds”.	1) Fractured quantum processes.
2) Multiphotonic processes of the creation CS.	2) Quantum reirradiated processes.
3) Quantum part of laser annealing of ion-implanted layers of semiconductors.	2. Second-order wave effects and here structures:
4) Photochemical processes.	1) All possible thermochemical processes and here structures.
2. First-order wave effects and here structures:	2) Plasmic wave processes.
1) Holograms.	3) “Frozen” diffraction and interferometers pictures.
	4) Wave part of laser annealing of ion-implanted layers of semiconductors.
	5) Reirradiated wave processes and its structures.

The basic parameters of quantum CS may be geometrical (concentration and size of basic elements of structure) and energize (energy of the

activation or energy of chemical bond). These parameters are the basic parameters of RO [34].

The classification of basic CS of RO according to classification basic phenomena of RO is represented in Table 3.

Table 3: The classification of basic CS of RO according to classification basic phenomena of RO [34]

Kinetic phenomena	Dynamic phenomena	Mixing phenomena
1) Creation "dangling bonds".	1) Holograms.	1) Impulse laser annealing of ion-implanted layers of semiconductors.
2) Multiphotonic processes of the creation CS.	2) All possible thermo-chemical processes and here structures.	2) Laser implantation of solid.
3) Quantum part of laser annealing of ion-implanted layers of semiconductors.	3) Plasmic wave processes.	
4) Photochemical processes.	4) "Frozen" diffraction and interferometers pictures.	
5) Fractured quantum processes.	5) Wave part of laser annealing of ion-implanted layers of semiconductors.	
6) Quantum reirradiated processes.	6) Reirradiated wave processes and here structures.	

The classification of coherent structures of Table 3 is more full and proper to basic experimental data of RO.

For example, CO_2-laser irradiation of $InSb$ in continuous regime with power density $\sim 30W \cdot cm^{-2}$ is caused of the sublimation the irradiated material [34]. It is laser pulverization of materials. It is multiphoton process. The quantum energy is less than band gap of the semiconductor. Therefore the basic first-order effect is the absorption on the free electrons. But for the regime of the saturation of the irradiation the processes of multiphotonic absorption and step-by-step self-absorption are basic. The next stage of these processes is the creation of the dangling bonds and the thermalization of the process. The process of hydro dynamization for these regimes of irradiation is absented. Basic cause of its is the ratio between the quantum energy (0,11 *eV*) and band gap (0,18 *eV*). The absence of the melting of the crystal may be explained with help of the quantum character of the interaction. Sublimation

is the result of short-range approximation of the interaction (multiphoton absorption and further ionization of material).

Fractured CS may be represented the subsurface layers which are created in $InSb$ and $InAs$ after Ruby laser irradiation (duration of irradiation $2 \cdot 10^{-8} s,$ density of energy in pulse $0{,}01 - 0{,}3 \ \ J/cm^2$) [31-36]. Quantum energy (1,78 e*V*) is more than band gap. For $InSb$ it is minimal energy of chemical bond in crystal (pure covalent bond). Next bond have value 1,95 *eV*. Therefore the basic partner of self absorption is the "band gap" bond. One quantum of Ruby laser may be created 3-5 electrons (near 3-5 covalent bonds).

The size of the place the determination of the awakening the quantum CS is determined of the size of corresponding chemical bond or lattice number $\left(10^{-8} cm \div 6 \cdot 10^{-8} cm\right)$. For wave CS this size is determined through the wave length $\left(10^{-5} cm \div 6 \cdot 10^{-3} cm\right)$. These estimations are characterized "soft" regimes of the irradiation.

Characteristics of wave coherence are the time and the length of the coherence. The time of coherence is determined from the Rayleigh relation [34]

$$\Delta t \Delta \nu \le 1, \tag{47}$$

Where $\Delta \nu$ -effective spectral width of the of retard irradiation.

The time of the coherence (coherence time) is the time [34]

$$t_{coh} = \Delta t = \frac{1}{\Delta \nu}. \tag{48}$$

The length of the coherence (coherence length) is determined as

$$l_{coh} = c \Delta t. \tag{49}$$

But these relation's are corresponded to wave optics only. Therefore time of the coherence may be represented as the time of the formation local centers of coherent structures and as the time of the disorder of irradiated structures.

For the formations "dangling bonds" structures we have to times of the coherence. First, the time of interaction light and covalent electron may be determined from uncertainty principle [34].

$$\tau_{in} = \frac{\hbar}{E_g}, \tag{50}$$

Where E_g -band gap of semiconductor. This time has value $3{,}7 \cdot 10^{-15} s$ for $InSb$ [34].

The problem of the transition from the covalent or another chemical bond to band gap is very important in modern physics and chemistry of solid. The first is the basic notion of physical chemistry, second-the physics of solid state. The "dangling covalent bonds" in crystal may be cause of irreversible change in solid (the creation of damages) and source of oscillation in lattice. The last may be created the irreversible changed in solid too. But times of the creation these damages of the lattice are various.

For short-range change (electromagnetic relaxation) this time may be determined according to next formula [34]

$$\tau_{er} = \frac{\Delta r}{\vartheta} = \Delta r \sqrt{\frac{M}{2E_g}}, \tag{51}$$

Where M is mass or reduced mass of semiconductor atoms; ϑ is speed of the atomic motion after break of covalent bond.

For long-range change (plasmic and thermal processes) the time of the coherence may be determined as time of the relaxation system (electromagnetic or thermal) to the state of the thermodynamic equilibrium. The corresponding length of the coherence may be determined trough diffusive length [34]

$$l_{pl} = \sqrt{D_{pl} t_{pr}} \text{ or } l_{th} = \sqrt{D_{th} t_{tr}}, \tag{52}$$

Where l_{pl}, l_{tr} -plasmic and thermal length of free range respectively; D_{pl}, D_{tr} -proper plasmic and thermal coefficients of the diffusion.

The one of the basic parameter for the creation of CS is the concentration of the excitation and centers of light scattering. The critical value of these parameters N_c must be correlated with time characteristics of corresponding processes [31-36]. For the creation coherent structures on the metastable structures (for example, ion-implanting layers of semiconductor) N_c is the concentration of damages (radiation defects) centers in irradiated

layers. In this case parameter of the coherence may be the critical value of the absorbed irradiation. Here volume density may be determined as

$$I_c = \frac{h\nu N_c}{n\left(1 - R_{refl}\right)}, \tag{53}$$

Where R_{refl} -reflection index of semiconductor, n -the quantum effectiveness of light absorption, l -the middle depth of the light absorption.

The mixed structures (quantum-wave and wave-quantum) may be created between quantum and wave CS. In quantum optics is the analogous effect of particular coherent light. But quantitative estimation of these effects is absented.

For the mixed structures and its evolution the parameter of order [31-36] may be used as the parameter of the coherence too. It is the system parameter and here has more thermodynamic nature as optical. But for the RO the parameter of order may be one of basic for the research of complex CS.

Wave CS may be classified as monowave or multiwave structures. In irradiated materials the diffraction picture may be frozen [31-36]. This picture may be have period of wavelength of using irradiation, second or third harmonic of its irradiation. For the irradiation with $h\nu >> E_g$ this period is caused of the irradiation with wavelength $\sim E_g$ (fractional wave CS). The possible explanation of these results may be next. The diffraction pictures for the regime of irradiation with $h\nu >> E_g$ may be created (frozen) the second-order effects of the irradiation: the result of the interaction heated crystal and relaxed inner radiation (the radiation with $h\nu \sim E_g$). Now the processes of the creation the fractured CS isn't researched almost.

The important problem for CS is the problem of the transition from the first-order phenomena of the interaction light and matter to the second-order effects (relaxed processes). These processes may be have various lifetimes. Therefore for the real processes we must know kinetic characteristics all possible second-order phenomena and its hierarchy.

The problem of stability CS has fundamental physical interest because the problem of the creation new stable centers of crystal or amorphous states of irradiated material and its theoretical representation are one of central problems of RO.

For the qualitative and quantitative modeling of CS must be used methods of molecular and atomic dynamics, statistical physics of irreversible phenomena, quantum optics and electrodynamics.

Perspective direction of the development theoretical research in this chapter physics is the using the coupled wave theory [31-367]. This theory may be synthesized with Volterra differential [31, 32] and other kinetic equations and other methods (Haken method [9, 31, 32], diffusive expansion [32] of Volterra equations) because we must represented wave and quantum part of the creation the CS.

More detail research of mixed effects of RO may be help determine the nature of wave-corpuscular dualism and transition between coherent and incoherent states and also between coherent states of various step of the coherence. This research may be help to determine the transition from quantum and wave coherent states. Basic difficulty for the modeling of this processes is the selection corresponding kinetic coefficients and the bond between one.

As rule the stable structures are produced for the light absorption in metastable matter. For stable matter stable CS may be received as threshold structures [31-36]. The problem of the modeling the threshold of the creation the stable or metastable states or phases in disordered and ordered materials hasn't full resolution and one is absented practically for CS.

The stability of coherent structures has great meaning for the creation new elements of electronics and optoelectronics. These structures may be have lifetime from $10^{-7}s$ to few years. For example, the irradiation in spectral range $h\nu < E_g$ may allow receiving new more stable CS with new physical and chemical properties as start material. The selection regimes of the irradiation may be caused of redistribution the impurities and basic atoms or atomic and molecular bonds in irradiated materials too.

The further research of the processes the creation, the evolution and the transformation of CS are necessity for the development of RO and its applications.

IV. Other applications theories of optical coherence

The problem of correlation of light and structural coherence is connecting with development of Nonlinear Optics [1-55], including holography [41-46, 48]. It are conditions of phase synchronism in NLO and coherence length in holography.

Conditions of phase synchronism in classic Nonlinear Optics (generation of second and higher orders harmonics, up and down conversion and other are characterizing of a values of angle of phase synchronism. Its values are changing from few dozens of angle seconds to few dozens of angle minutes [12]. In this case, we have resonance phenomena [12].

The problem of diffraction and self-diffraction processes in Nonlinear Optics (NLO) and Relaxed Optics (RO) has long history [31-36]. Roughly speaking NLO phenomena are conducted with RO processes (aging of irradiated materials and basic NLO elements and devices).

The question about nonequilibrium laser-induced diffraction gratings were analyzed in dynamic holography [37]. Diffraction is connected with self-trapping too [31-36]. Self-trapping is result of equivalence self-focusing and diffraction [34].

These problems have large value in RO [31-36]. Methods of RO are used for the creation new laser technologies for the creation nano and microstructures [31-36]. So, laser-induced surface, interferograms may be explained with help Makin plasmon-polariton concept [31-36]. But microstructure of these interferograms of nano and micro columns can't observe with help of this concept. One of possible mechanism of this phenomenon may be formation of surface diffraction grating. In this case we have two processes: wave processes of creation interferograms and local processes of creation frozen diffractogram, which is modulated by interferograms. This fact may be explained with help physical-chemical cascade theory of excitation proper chemical bonds in the regime of saturation the excitation [33, 34].

For use focused laser radiation in impurity range of absorption spectrum of irradiated matter we can have next scenario [36]. Firstly is diffraction layering; secondly after further focusing no layering irradiation we have generation cascade of Cherenkov radiation [34, 36] (for experimental data, which are represented in [34, 36], 5-stages cascade of laser-induced destruction of silicon carbide; thirdly this Cherenkov radiation is caused of creation frozen channels of optical breakdown. In this case we can represent observed experimental data as creation of irreversible diffraction grating too.

The processes of nonequilibrium and irreversible changes in laser-irradiated matter may be represented with point of theory of phase transformations. So, basic classical nonlinear optical phenomena may be represented as nonequilibrium second order phase transitions according by H. Haken [34]. The irreversible laser-induced phase transformations have larger spectrum [31-36].

The problem of diffusion and self-diffusion processes in Nonlinear and Relaxed Optics wasn't research in whole, therefore this paper allow to represent this problem as autonomous problem.

Conditions of phase synchronism are the conditions of spatial and temporal coherence in Nonlinear Optics. In this case, we must have generation of resonance homogeneous polarization. The example of Nonlinear Optical phenomena with heterogeneous polarization is optical-induced Cherenkov radiation [36]. Cherenkov radiation may be represented as radiating relaxation of optical-induced heterogeneous polarization of matter [36]. Conditions of coherence for Cherenkov radiation have more complex nature as for classic Nonlinear Optics [36].

In 1891, G. Lippmann demonstrated a method of obtaining colorfastness photographs. The process for obtaining color photographs was proposed in 1848 by the French physicist E. Becquerel. It used a silver plate covered with a layer of silver chloride, but the photographs quickly faded, and Becquerel himself could not explain the formation of the color image. 20 years later, German physicist W. Zenker explained the appearance of color in Becquerel's photographs by the phenomenon of interference. Zenker's theory was further developed in the works of the English physicist J.W. Strutt and was experimentally confirmed in 1890 by the German physicist O. Wiener [43].

Interference is nothing more than a combination of different light waves arriving simultaneously at the same point. Light is an electric and magnetic field, the intensity of which periodically increases, decreases and changes sign along the axes perpendicular to each other and the direction of light propagation. Therefore, light waves can strengthen or weaken each other, depending on whether their fields are directed in the same direction or in opposite directions. If the light waves have the same length (and the corresponding frequency), then an interference pattern appears-rings or stripes. Bright spots on it correspond to the arrival of waves in phase (at the same point of the complete cycle of change), dark spots-to the arrival of waves in antiphase (at diametrically opposite points of the cycle). The distance between spots in the interference pattern depends on the wavelength. Waves with different wavelengths, interfering, create patterns that move relative to each other continuously, as a result of which the overall picture is blurred.

On Becquerel photographic plates, Zenker explained, the incident light interferes with light of the same wavelength reflected from the silver plate,

which creates a picture of bright layers located at half-wave intervals and separated by dark layers. Since the wavelength corresponds to the color perceived by the eye, different colors create interference patterns at different depths and in different places on the plate where they occur with incident light. The light energy accumulated at each point of the film during the exposure determines the number of grains of metallic silver that are formed from silver chloride during the subsequent development of the plate. These metal grains become copies of the interference patterns for different colors as darkened layers located at different depths and with different lateral displacement.

When viewing such a photograph in ordinary light, i.e. in a mixture of all colors, light is reflected both from the layers of grains of metallic silver and from the silver-plate itself. Light waves reflected from layers of different depths are amplified, because of interference only at a very specific wavelength (color) corresponding to the distances between the layers, and thus reproduce the colors of the photographed object.

When G. Lippmann invented his method of color photography, which made it possible to obtain pictures that did not fade soon after development, he denied that the colors in photographs according to the Becquerel method were due to interference. L. argued that interference lies at the heart of his own method. Lippmann plates were made of transparent glass and covered on one side with a relatively thick layer of light-sensitive emulsion of gelatin, silver nitrate and potassium bromide. During the exposure, the cassette covered the free side of the glass plate with mercury, which created a shiny reflective surface. Interference patterns between the light falling from the object and reflected from the mercury (it is these interference patterns that store the “memory” of the color of the image), were imprinted in the distribution of silver grains that appeared because of chemical reactions during manifestation. Subsequently, Lipmann figuratively described the process invented by him as the creation of a kind of template or form, from light rays in the thickness of the photographic film [43].

G. Lippmann noted the need for further improvement of his method: “The exposure time (1 minute in sunlight) is still too long for portrait photography. When I first started working, the duration of the exposure reached 15 minutes. The process should be improved further. Life is short and progress is so slow. Modern color photography with films requiring a fraction of a second is based on a three-color process using absorbent dyes, first proposed in the 1950s. XIX century. Scottish physicist J.C. Maxwell [43].

Lippmann very ingeniously managed to combine the phenomenon of light interference with the capabilities of black and white halogen-silver photography (Fig. 2 a)) [43]. The image in the Lippmann camera was focused on a glass photographic plate, which was placed with an emulsion on the surface of mercury, which played the role of a mirror. The light first passed through the emulsion from top to bottom, and then, reflecting from the mercury, formed a standing wave in the emulsion, the period of which depended on the wavelength of light. So, the blue rays in the figure on the left formed a standing wave, the distance between the zeros of which (nodes) is less than the corresponding distance for the red rays on the right. Of course, in the nodes of the standing light wave, the latent image was not formed, but in the places of the maximum of the standing wave (antinodes), the maximum illumination occurred, which, after developing into a system of parallel stripes of metallic silver with gaps between the stripes corresponding to the wave of the color that irradiated in this place photo emulsion.

As a method of color photography, Lippmann's method lost out to additive color photography, but it became the forerunner of the method for obtaining color holograms proposed by the Soviet physicist Yu. N. Denisyuk after the appearance of sources of powerful monochromatic radiation-lasers (Fig. 2 b)) [46]. In fact, Lippmann's color photography is a Denisyuk hologram for a flat object, which is a picture focused on the surface of mercury the latter becomes obvious if you carefully look at the two diagrams explaining the reception of a hologram according to Denisyuk and the subsequent examination of the object with the help of Denisyuk hologram.

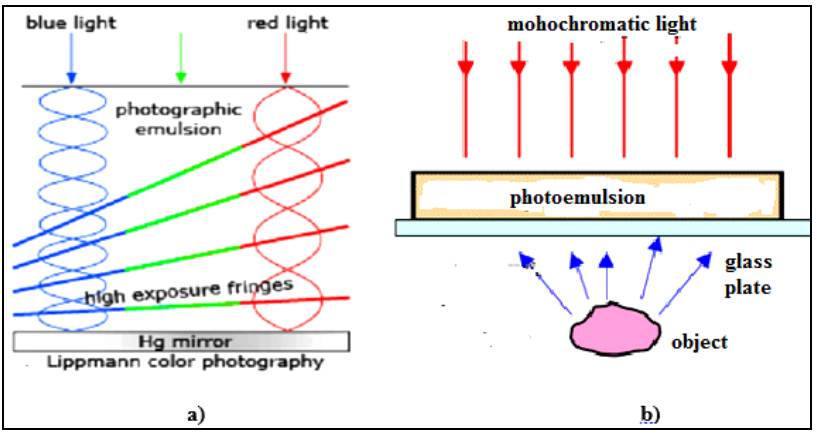

Fig 2: a) Lippmann scheme of receiving the color photography, b) Denisyuk scheme of receiving the volume holograms

The role of structural coherence in the formations of holograms was researched in [41]. It was shown, that increasing of excitation time of irradiated matter with first laser beam, allow made more soft conditions for the coherent properties of second laser beam.

If Denisyuk hologram is made three times using primary monochromatic radiation of three primary colors, then a color hologram will appear, and only a black-and-white result of interference will be recorded in the photographic emulsion. To record such holograms, special high-resolution (up to 5000 lines per millimeter) photographic emulsion has been developed. At the same time, it turned out that such emulsions have an extremely low photosensitivity (they can be irradiated with bright sunlight for a few seconds without fear of exposure), therefore, only recording can be carried out using an intense laser beam [46].

D. Gabor created holography for the resolution problems of increasing resolving power of the electron microscopy [29]. He created classical scheme of two-beams holography. Further this method was developed for radio waves by E. N. Leith and his colleagues and laser irradiation by E. N. Leith and J. Upatnieks [29]. These holograms were one and two-dimensional, Denisyuk three-dimensional [29, 46].

Other applications optical coherence are: laser physics [1, 18, 20, 26, 49], optical solitons [22, 24], self-focusing and self-trapping and problem of energy transitions on large distances [12, 30, 34, 36], researching of nonlinear fibering optics and creation fibering and non-fibering optical systems of communications [7], increasing resource and lifetime of basic elements of optoelectronic systems and new optical, including laser, technologies [31-36].

V. Conclusions

1) Basic concepts of optical coherence are analyzed.
2) Foundation classic theory of coherence is represented.
3) Basic notions of Quantum theory of coherence are observed,
4) Necessary of creation theory of coherent structures and its role in the creation of Relaxed Optics are discussed.
5) Short comparative analysis of resonance classic “monochromatic” nonlinear optical phenomena (generation of harmonics, up and down conversion etc.) and continuous optical-induced Cherenkov radiation is observing.
6) History of development the G. Lippmann color photography and holography with of view the coherence theory made too.

7) Main areas of application the represented concepts and theories of coherence in modern physics are analyzed too.

Acknowledgements

Author wishes to thank by M. Romanyuk, Ya. Dovhyy, L. Laz'ko, A. Tsaryk, A. Krochuk, O. Vlokh, Yu. Denysyuk, V. Bonch-Bruevich, P. Danylchenko, I. Stoyanova, P Eliseev for the discussion of basic questions and problems of coherence; and V. Holoviy, O. Viligurskyy, M. Shevchuk (Maydanovych) and D. Shvalikovskyy for help in the preparation of this work.

References

1. Perina J. Coherence of light. Moscow: Mir Publisher, 1974, 368.
2. Perina J. Quantum statistics of linear and nonlinear optical phenomena. Moscow: Mir Publisher, 1987, 370.
3. Glauber RJ. Quantum Theory of Optical Coherence. Selected Papers and Lectures. New-York A.A.: Wiley@Sons, 2006, 698.
4. Clauder JR, Sudarshan ECG. Fundamentals of quantum optics. Moscow: Mir Publisher, 1970, 428.
5. Mandel L, Volf E. Optical Coherence and Quantum Optics. Moscow: Fizmatlit, 2000, 895.
6. Akhmanov SA, Hohlov RV. The problems of Nonlinear Optics. Moscow: Nauka, 1964, 298.
7. Agraval G. Nonlinear fibering optics. Moscow: Mir, 1996, 324.
8. Akulin VM, Karlov NV. Intensive resonance interactions in Quantum Electronics. Moscow: Fizmatlit, 1987, 312.
9. Haken H. Laser light dynamics. Moscow: Mir, 1988, 350.
10. Andreev AV, Emelyanov VI, Il'ynskiy Yu. A. Cooperative phenomena in optics. Moscow: Nauka, 1988, 286.
11. Bloembergen N. Nonlinear Optics. Moscow: Mir, 1966, 424.
12. Shen J. Principles of Nonlinear Optics. Moscow: Nauka, 1979, 559.
13. Boyd RW. Nonlinear optics. Amstertdam a.o.: Academic Press, 2003, 578.
14. Carruthers P, Dy KS. Coherent states and irreversible processes in anharmonic crystals. Phys. Rev. 1966; 147(1):214-222.

15. Caulfield HJ. Handbook of Optical Holography. Moscow: Mir Publisher, 1982, 736.
16. Chang WSC. Principles of lasers and optics.-Cambridge: University Press, 2002, 262.
17. Dmitriyev VG. Nonlinear optics and phase conjugation. Moscow: Nauka, 2003, 256.
18. Eliseev PG. Introduction to physics of injection laser. Moscow: Nauka, 1983, 296.
19. Gorban AN. Optics. Kyiv: Vyshcha Shkola, 1979, 224.
20. Gribkovskiy VP. Semiconductor lasers. Minsk: University Press, 1988, 304.
21. Kielich S. Molecular nonlinear optics. Moscow: Nauka, 1981, 671.
22. Kivshar Yu S, Agraval GP. Optical Solitons. From fibers to photonic crystals. Moscow: Fizmatlit, 2005, 648.
23. Kushnir O, Korchak Yu, Lutsiv-Shumskiy L, Rykhlyuk S. Experimental optics. Lviv: Ivan Franko University Press, 200, 466.
24. Maimistov AI, Basharov AM. Nonlinear optical waves. London: Kluwer, 1999, 658.
25. Miloslavskiy VK. Nonlinear Optics. Kharkov: Karazin University Press, 2008, 312.
26. Piecara AH. Nowe oblicze optyki. Wprowadzenie do elektroniki kwantowej i optyki swiatla spolnego. Warszawa: PWN, 1968, 262.
27. Scully MO, Zubairy MS. Quantum Optics. Cambridge: University Press, 1997, 652.
28. Vinetskiy VL, Kuhtaryev NV. Dynamic holography. Kiev: Naukova Dumka, 1983, 127.
29. Gabor D. Holography (1948-1971). Adv. Phys, Sc. 1973; 109(1):5-30.
30. Self-Focusing: Past and Present. Eds. Boyd RW, Lukishova SG, Shen YR, Springer Series: Topics in Applied Physics, -NY: Springer. 2009; 114:605.
31. Trokhimchuck PP. Foundation of Relaxed Optics. Lutsk: Vezha, 2006, 294.
32. Trokhimchuck PP. Foundations of Relaxed Optics. Lutsk: Vezha, 2011, 627.

33. Trokhimchuck PP. Relaxed Optics: Realities and Perspectives. Saarbrukken: Lambert Academic Press, 2016, 260.

34. Trokhimchuck PP. Relaxed Optics: Modelling and Discussions. Saarbrukken: Lambert Academic Press, 2020, 249.

35. Trokhimchuck PP. Nonlinear and Relaxed Optical Processes. Problems of Interactions. Realities and Perspectives. Lutsk: Vezha-Print, 2013, 280.

36. Trokhimchuck PP. Laser-induced optical breakdown of matter: retrospective and perspective. Advances in Engineering Technology, part 7. New Dehly: AkiNik Publications. 2020; 4:101-132.

37. Changh Zenghu. Fundamentals of Attosecond Optics. Orlando: CRC Press, 2011, 506.

38. Csele M. Fundamentals of light sources and laser. New York a.o.: A John Wiley & Sons, Inc., 2005, 344.

39. Zewail AH. Femtochemistry: Recent progress in studies and control of reactions and their transitions states. J Phys. Chem. 1996; 100(31):12701-12724.

40. Ziętek B Optoelektronika. Toruń: Wydawnictwo universytetu Nikolaja Kopernika, 2005, 615.

41. Arkhipov RM, Arkhipov MV, Rozanov NN. On the possibility of holographic recording in the absence of mutual coherence of the reference and object beams. JETP Letters. 2020; 111(9):596-600.

42. Petrov M, Stepanov S, Homenko A. Photorefraktive cristalls in coherent optics. Moscow: Nauka, 1992, 159.

43. Judd D, Wyszecki G. Color in science and engineering. Moscow: Mir, 1978, 592.

44. Soroko LM. Foundations of holography and coherent optics. Moscow: Nauka, 1971, 616.

45. Collier RG, Burckhardt DT, Lin LH. Optical holography. Moscow: Mir, 1973, 688.

46. Denisyuk Yu N. Principles of holography. Lectures. Llnigrad: Sergey Vavilov optical institute, 1979, 126.

47. Newton I. Optics: or a Treatise of the Reflections, Refractions, Inflections and Colors of Light. 4-th edition. London: Printer for William Innys at the Welt-End of St. Paul's, 1730, 386.

48. Kock WE. Lasers and holography. An introduction to coherent optics. Moscow: Mir, 1971, 137.

49. Popescu IM, Preda AM, Cristescu CP, Sterian PE, Lupaşcu AL. Probleme rersolvate de fizica lazerilor. Bucureşti: Editura technical, 1975, 443.

50. Born M, Volf E. Principles of Optics. Oxford a. o.: Pergamon Press, 1986, 854.

51. Rayleygh (Strutt JW). Wave theory of light. Strutt JW (Baron Rayleygh). Scientific Papers, Cambridge: University Press. 1902; 3:47-189.

52. Romanyuk MO, Krochuk AS, Pashuk IG. Optics. Lviv: Ivan Franko National University Press, 2012, 564.

53. Romanyuk MO. Crystall Optics. Lviv: Ivan Franko National University Press, 2017, 456.

54. Bohr N. The quantum postulate and the recent development of atomic theory. Nature. Supplement. 1928; 121:105-143.

55. Françon M, Slansky S. Coĥerence en Optigue. Paris VII: Ėditions du centre national de la recherché scientifique, 1965, 80.

56. Einstein A. To the modern state problems of specific heat capacity. A. Einstein. Collected scientific papers, vol.3. Moscow: Nauka, 1966, 277-313

57. Martynov D. Ya. Practical Astrophysics Course. Moscow: Nauka, 1977, 544.

Chapter - 2
Design of MIMO Microstrip Patch Antenna for 5g Applications

Authors

S. Nithya
Assistant Professor (Sr. G), KPR Institute of Engineering and Technology, Coimbatore, Tamil Nadu, India

M. Manikandan
Application Engineer, Crestron Electronics, Bangalore, Karnataka, India

M. Singaram
Assistant Professor (Sr. G), KPR Institute of Engineering and Technology, Coimbatore, Tamil Nadu, India

A. Reethika
Assistant Professor, KPR Institute of Engineering and Technology, Coimbatore, Tamil Nadu, India

V. Chandraprasad
Assistant Professor (Sr. G), KPR Institute of Engineering and Technology, Coimbatore, Tamil Nadu, India

Chapter - 2

Design of MIMO Microstrip Patch Antenna for 5g Applications

S. Nithya, M. Manikandan, M. Singaram, A. Reethika and V. Chandraprasad

Abstract

Now a day, extensive research on the 5G technology is on the rise. With the commercialization of fifth-generation (5G) mobile communication, high-bandwidth communication and smart wireless services are approaching. Here, an eight-element broadband MIMO (Multiple Input Multiple Output) array with high element insulation enrichment for metal-framed 5G smart phones is presented. The 4x4 MIMO microstrip antenna which provides excellent results with S parameter less than -10db, VSWR less than 2 and efficiency of 80%. The designed MIMO antenna array comprises resonators as insulating element. To improve the bandwidth, the required resonances can be obtained by adjusting the slots.

Keywords: 5G, MIMO antenna, high isolation

I. Introduction

Future wireless networking technology would necessitate a much smaller antenna due to the exponential growth of wireless technology. In the field of wireless systems, antennas play a critical role. Because of its large size and 3D geometry, the basic antenna is known widely and used in many applications but, it doesn't meet all the requirements. Thus slowly arises MIMO antenna. One of the most exciting features of 5G is the MIMO antenna. MIMO technology can increase data transfer speeds while also providing multi-method resistance to fading. This MIMO device has proven its ability to enhance spectral communication efficiency across a wide range of applications.

Method

MIMO technique

This MIMO method has been commonly used because it accepts a broad volume and number of connected devices. The MIMO antenna is

multilayered with integrated 5G network. Transmitter or receiver in a MIMO antenna needs two or more antenna components. MIMO refers directly to the efficient process of transmitting and receiving multiple signal data at a time over the same station by exploiting multipath broadcasts. MIMO brings solution to deal with challenges. This technology, which increases the volume by transmitting different signals to multiple antennas

1X1 Antenna

The below Figure 1 shows the 1x1 microstrip patch antenna. It comes under microstrip patch antenna type. This single antenna has ground as their base, over the ground dielectric substrate will be placed, and above the dielectric substrate patch will be placed. With the reference of below antenna, 4x4 MIMO antenna will be designed.

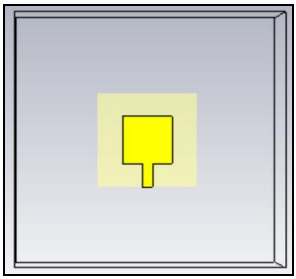

Fig 1: 1x1 Antenna structure

2X1 Antenna

The 2x1 MIMO, for example, displays two antennas at the end of the transmission and two antennas at the end of the acquisition, the minimum required for a standard 802.11n frame. At the end of the discovery, each antenna detects a different mix of signal streams.

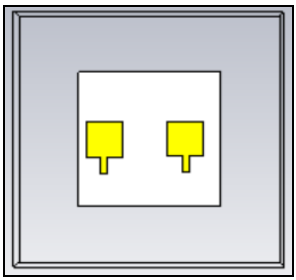

Fig 2: 2x1 Antenna structure

Software tool

CST MICROWAVE STUDIO® (CST MWS) is a 3D electromagnetic simulation tool for high-frequency applications. Horns, filters, couplers, and

multi-layer systems are examples of high frequency (HF) devices. Results, can all be analyzed easily and reliably with CST software. CST is followed by the finite integration technique (FIT), which explains Maxwell's equation on a grid arrangements and is common among antenna designers since simulations are easy.

Design methodology

It is a rectangular shaped, low profile antenna. It is made up of a large metal plate known as a ground plane and a rectangular piece of metal.

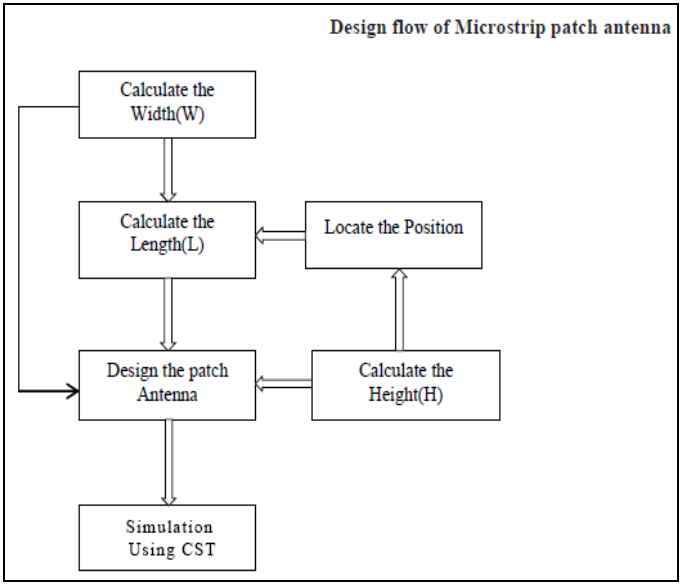

Fig 3: Design flow

Substrate

The substrate is placed between rectangular wing and the ground plane. There are an excessive number of substrate materials to choose from. FR4 epoxy is what working with. It has a dielectric loss tangent of 0.02 and an average clearance of 4.4. FR4 is a strong microwave substrate with low dielectric loss. The substrate in a microstrip antenna is used to support the antenna mechanically and electrically.

A microstrip antenna's radiation pattern and impedance bandwidth are also affected by its dielectric loading. As the antenna bandwidth decreases the dielectric increases continuously, increasing the antenna's Q factor and lowering the impedance bandwidth. When using an antenna transmission line model, this relationship did not emerge right away. For a rectangular

microstrip antenna. identical slot pairs are used. If an antenna has dielectric as air, these particles behave as parallel components with a very high path, which decreases when it is replaced by a dielectric substrate, resulting in a higher allowance.

A transparent defect plane is visible in the middle of a rectangular microstrip antenna. To make a quarter-wavelength microstrip antenna, this can be replaced with a shorter aircraft. This is can be denoted as a half-patch. The antenna has a single radiation edge, which decreases antenna's path. As the light edges junction is eliminated, the bandwidth impedance is slightly lower than the maximum half-wavelength patch.

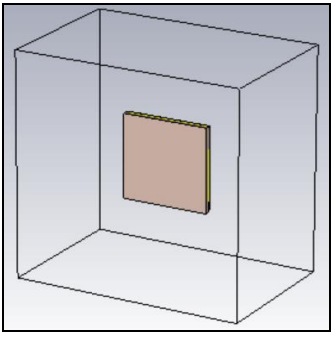

Fig 4: Substrate

Antenna design

Initially, the ground plane is designed and then the antenna is mounted on it. Continuously, we fed supply to the antenna. This antenna is operated using a high frequency (CST) structure.

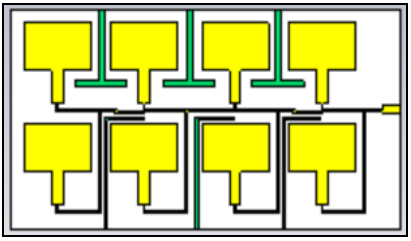

Fig 5: 4x4 MIMO

The above figure shows the 4x4 MIMO antenna with T shaped resonators shaped resonators is introduced to avoid mutual coupling between each and every antenna element.

Results and Discussion

Simulation results

Simulation results are used to understand the performance of the antenna. The simulator CST STUDIO gives effective bandwidth and better efficiency. This simulator is useful for reducing false costs.

S-Parameter

S-parameter describes the input-output relationship between ports in an electrical system. Since the network changes both the size and the signal phase of the case, S-parameters are complex numbers of real and imaginary parts or dimensions and phase components. The reflection coefficient achieved is less than -6dB. The antenna is radiating at the two different frequencies in 4.7 GHz and 5.8 GHz. These multiple frequencies make the antenna to work in larger bandwidth and provide the better gain and directivity.

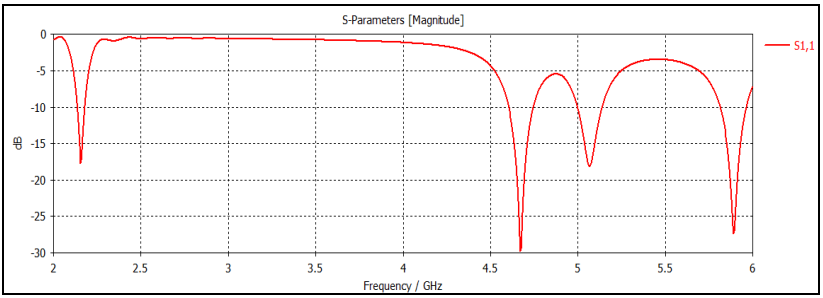

Fig 6: S Parameter

VSWR

It is a measurement of the quality of radio frequency energy as it travels from a source to a transmission line and then to a feed line. 100 percent power is transferred in the correct method if VSWR value lies below 2. The below figure 8 shows the VSWR of the 4x4 MIMO antenna, this shows the VSWR value as less than 2 the two different frequencies in 4.7 GHz and 5.8 GHz.

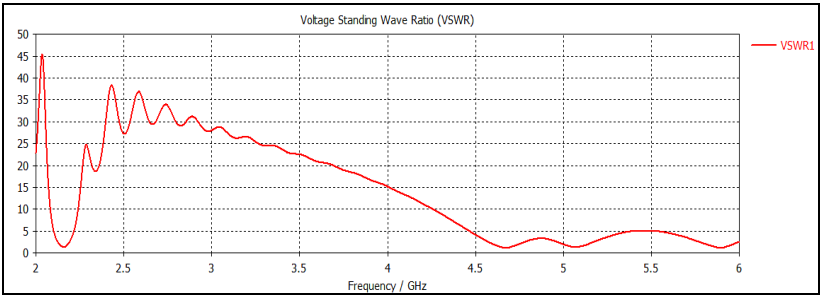

Fig 7: VSWR

Radiation pattern

Radiation pattern (also known as antenna pattern or far-field pattern) is a concept used in antenna design to describe the directional (angular) dependence of the frequency of radio waves emitted by an antenna or other source, for example, can compute the near field using other applications.

Far field

The far field behaves like "natural" electromagnetic radiation. As the square of distance in the far-field area of an antenna, decreases the power. The absorption of the radiation does not feed back to the transmitter.

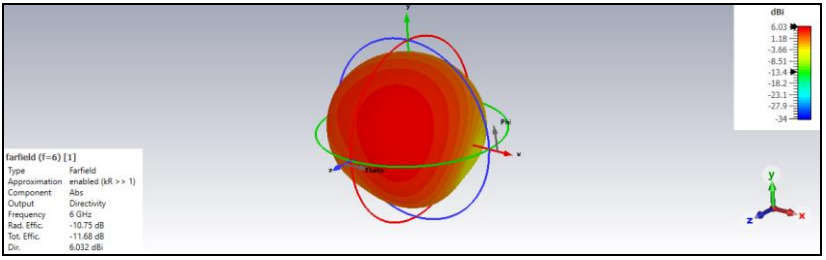

Fig 9: Far Field Pattern

Conclusion

A rectangular microstrip antenna is designed using CST software. This MIMO antenna is simulated for wideband frequencies. Here the designed antenna radiates at two different frequencies like 4.7 GHz and 5.8 GHz. The data rate will be faster in this 5G network compared to the 4G version. Here achieved 78% efficiency. In addition, performance is always less honorable the result caused by the hands of the user in place call applications.

References

1. Karuna Kumari K, Sridevi PV. Design and Analysis of Microstrip Antenna Array Using CST Software, International Journal of Engineering Science and Computing, 2016, 6.

2. Mowafak K Mohsen, Isa MSM, Rahman TA, Abdulhameed MK, Isa AAM, Zin MSIM *et al*. Novel Design and Implementation of MIMO Antenna for LTE Application, Journal of Telecommunication, Electronic and Computer Engineering, 10.
3. Xiao-Ting Yuan, Wei He, Kai-Dong Hong, Chong-Zhi Han, Zhe Chen, D Tao Yuan. Ultra-Wideband MIMO Antenna System with High Element-Isolation for 5G Smartphone Application, IEEE Access, 2020, 8.
4. Tommi Hariyadi, Rizky Permadi Megantara. Directional 2X2 MIMO Microstrip Antenna Design and Optimization for LTE Band-3 Application, ICITACEE, 2018, 9.
5. Gurpreet Singh, Ajni Anjit, Singh Momi. Microstrip Patch Antenna with Defected Ground Structure for Bandwidth Enhancement, International Journal of Computer Applications, 2013, 73.
6. Imran D, Farooqi MM, Khattak MI, Ullah Z, Khan MI, Khattak MA *et al*. Millimeter Wave MicroStrip Patch Antenna for 5G Mobile Communication, International Conference on Electronics Engineering and Technology, 2018.
7. Madhan MD, Subitha D. Millimeter-wave Microstrip Patch Antenna Design for 5G, International Journal of Innovative Technology and Exploring Engineering, 2019, 8.
8. Pooja Siriya JA, Shrawankar SS. Balpande Design and Development of Inset Feed Microstrip Patch Antennas using Various Substrates, International Journal of Innovative Technology and Exploring Engineering, 2019, 8.
9. Surajo Muhammad, Abdulmalik Shehu Yaro, Isiyaku Ya'u AT. Salawudeen. Design of 5g Mobile Millimeter Wave Antenna, Journal of Science, Technology & Education, 2019, 7.

Chapter - 3
A Review on Identifying the Underground Cable Fault

Authors

S. Nithya
Assistant Professor (Sr. G), KPR Institute of Engineering and Technology, Coimbatore, Tamil Nadu, India

M. Singaram
Assistant Professor (Sr. G), KPR Institute of Engineering and Technology, Coimbatore, Tamil Nadu, India

A. Reethika
Assistant Professor, KPR Institute of Engineering and Technology, Coimbatore, Tamil Nadu, India

V. Chandraprasad
Assistant Professor (Sr. G), KPR Institute of Engineering and Technology, Coimbatore, Tamil Nadu, India

Chapter - 3

A Review on Identifying the Underground Cable Fault

S. Nithya, M. Singaram, A. Reethika and V. Chandraprasad

Abstract

Underground cables are being employed extensively in our country for the past few years. The underground cables can encounter damages due to several factors. Some of the factors being moisture entering the insulation, damages during transportation, wear and tear, poor man labour during installation these damages causes and electrical fault in the cable. A fault in an electrical equipment is defined as a change in the path of electricity from its intended path. Unlike in the over head transmission lines, in underground cables detecting the source of fault manually is difficult as we would have to dig up the whole cable. This chapter provides us with a solution to find out the exact distance of fault in the cable from the base station in kilometers. Our proposed model uses the very simple concept of v=ir, that is the principle of ohm's law to detect the fault. Here when the voltage is applied to circuit the value of current changes depending on the location of fault. So, in case of a short circuit the voltage measured across the resistor is passed to the Arduino's analog to digital converter pin. The Arduino then processes this data and the fault is displayed in terms of distance from the base station on the liquid crystal display (LCD). Using our proposed methodology we can locate the fault and dig up only that particular affected area instead of the whole cable. This saves a lot of time, money and man labour.

Keywords: fault, arduino microcontroller, liquid crystal display, ohm's law

1. Introduction

In India majority of power transmission cables are over-head cables. These over-head cables are prone to a lot of damages due to rainfall, snowfall, lightning, thunder also heavy automobiles can severe the overhead cables. This is one of the reasons why we are shifting to underground cables for power transmission in many places which are frequently prone to these climatic effects. But even underground cables have their fair share of damages which are caused due to wear and tear, rodents, poor handling and

transportation, poor installation etc. Though the frequency of damage occurring in underground cables compared to overhead cables are less, the time and cost involved in the repairing the underground cables is more if the exact point of the fault is not located. To overcome these problems involved in the underground cable we have proposed a very simple yet efficient method of fault localization in this chapter. Our proposed method uses the concept of ohm's law. Basically the fault in an electric circuit can be broadly classified into two types:

1) **Short circuit fault:** Short circuit fault occurs when current bypasses the normal load. These are one of the most commonly occurring faults wherein an abnormally high current passes through the transmission cable. If allowed to persist they may cause extensive damage to the equipment.
2) **Open circuit faults:** These faults occur due to failure of conductors. In open circuit fault there is no complete loop for the current to flow in due to severed connection hence the current will be zero, that is I = 0.

2. Literature review

Jingbo Yuan, Jisen Zheng, Shunli Ding has developed study of pattern matching algorithm [2]. They have proposed this approach for fast intrusion detection using BM algorithm. Zakareya Laser, Sai Shiva VNR Ayyalasomayajula and Khaled Elleithy, has proposed an approach on epilepsy seizure detection using EEG signals [1]. They developed a system in which the EEG signals are processed both in time and frequency domains and applied a Chebyshev for pre-processing the signal. Jessica J. Falco-Walter, Ingrid E. Scheffer Robert, S. Fisher, have developed an research on classification of seizures and epilepsy and how these classifications may impact patients, doctors and clinicians [3].

Qi Yuan, Weidong Zhou Liren Zhang, Fan Zhang, Fangzhou Xu, Yan Leng, Dongmei Wei, Meina Chen, has developed an approach based on imbalanced classification existing in seizure detection which is addressed by weights ELM [4]. The WPT is used to decompose EEGs, and obtain time and frequency domain features. Yusuf U Khan, Omar Farooq and Priyanka Sharma extracted two statistical features i.e. skewness and kurtosis with a wavelet-based feature from the data and the classification between normal and seizure EEGs was performed using simple linear classifier [8]. Pallavi Lokhande and Tushar Mote are sending an SMS to doctor and parents as soon as the fits start as well as an SMS when the FIT ends. The main idea of

the epilepsy monitoring and analysis system using android platform is to monitor and analyze the Epilepsy attack and also track the progress of patient with in a given period of time [6].

P. Grace Kanamni Prince, Rani Hemamalini and R. Immanuel Rajkumar used accelerometer MPU6050 to acquire the signals from the extremities to detect abnormal movements and sudden fall of the epilepsy seizure patients. The Wavelet transform is used for detecting the changes in movement of the extremity and a thresholding technique is used for seizure detection and fall detection [7]. Shivani Tiwari, Varsha Sharma, Mubarak Mujawar, Yogendra Kumar Mishra, Ajeet Kaushik and Anujit Ghosal have proposed a system for detecting epileptic seizures by the use of biosensors. The system mainly uses advancements in state-of-art biosensing technology for epileptic diseases diagnostics and continuous monitoring or sometimes used for both the purposes. The system approximately uses 4 sensors such as EEG, ECG, EMG, ECoG which continuously monitors the body conditions of the patients thus greatly helps in epilepsy management [9].

IoT platform for monitoring and supervising system was developed by Paula M. Vergara, Enrique De La Cal, Jose R. Villar, Victor M. Gonzalez, and Javier Sedano [11] which mainly focuses on two main types of epilepsy the focal myoclonic and the epileptic absence seizures. The system uses tuned and trained models of previous existing system into the MCC kernel which allows continuous monitoring and providing real time responses through Wi-Fi Networks. Another which was developed by Ahmed I. Sharaf, Mohamad Abu El-Soud and Ibrahim M. El-Henwy was based on Q-Wavelet and firefly feature selection algorithm [10] the tunability of the Q-factor provides a proficient method to adopt wavelet transformation and the firefly algorithm which is a stochastic search technique.

3. Hardware description

3.1 Arduino microcontroller

A microcontroller is a mini computer like device which is built on a single metal oxide semiconductor integrated circuit. A microcontroller comprises of one or more central processing unit along with input output peripherals and memory devices. In our project we are using Arduino uno microcontroller. Arduino Uno is a ATmega328p based microcontroller. It comprises of 14 digital input/output pins, a 16 MHz quartz crystal, a USB connection, a power jack, an ICSP header and a reset button, 6 analog inputs. We can very easily connect it to a computer and other device peripherals with a USB cable and power it with a AC-to-DC adapter or battery to get

started. Arduino uno is a widely used for small scale experiment purposes as in case of any damage we can easily replace the chip. Hence the cost of damage repair is very minimum. Also because of the advanced added features which are in build with the microcontroller we can reduce the cost of adding special peripherals to the microcontroller like analog to digital converter etc. The Arduino uno has a special customized architecture based on the Harvard architecture with 8-bit RISC processor. It offers an UART serial communication with the transmission and reception pins TX (1) and RX(0). The Arduino board can be programmed with the Arduino programming language. The advantage of Arduino uno is, it is cheap and easily affordable, there is no need for an external programming, also it is an open source platform in both hardware and software. fig. 3.1.

Fig 3.1: Arduino Microcontroller

3.2 GSM Module

The GSM is abbreviated as the Global System for Mobile Communications, it is a standard developed by European telecommunication standards institution. The GSM is a hardware device that is a mobile or modem-based device that allows a computer to communicate over any network. In other words the GSM module provides data link or internet access to the remote operating device or the remote network. The GSM standards were laid down to describe the protocols for 2G cellular data for mobile phones. The GSM module consists of communication interfaces like RS-232, USB 2.0 and a power supply port for its operation with a connected device. The GSM/GPRS modules differ from the GSM/GPRS modems in the fact that the modules can be integrated with the devices whereas the modems are externally connected devices. Hence the GSM/GPRS modules reduce the device complexity. The wireless communication happens through the process of generating, transmitting or decoding data from the cellular network to establish communication. For this purpose all the GSM/GPRS

modems use a SIM card just like mobile phones to activate the communication link. The GSM module can perform all the function of a mobile phone like sending and receiving messages through the computer using the AT command.

Fig 3.2: GSM Module

3.3 Handheld current transformers

A current transformer is a device used to step up or step down, that increase or decrease the current in the coil. The transformer has a primary coil in the input side and a secondary coil in the output side. The current produced in the output is proportional to the current in the primary coil. The transformers are useful in differentiating high values of current and voltage and hence helps in protecting current and voltage sensitive devices from short circuit faults. These are currently used in all industrial applications like in power generation units, electrical substations etc. for sensing current units. A handheld current transformer also called as a clamp meter can be used to measure the circuit loading. It provides a very efficient and quick reading of the current measurements usually in the digital format when placed around the current carrying conductor without rupturing the connection of the conductor or opening the connection. The handheld current transformers can measure current in the range of 100up to 5000 amps. The handheld current transformer works on the principle of producing a magnetic flux proportional to the current in the primary coil of the transformer. This magnetic flux then induces a proportional current in the secondary coil. The handheld current transformer is used in our project to interface the current from the source to the protective relay in the required measuring units.

Fig 3.3: Temperature Sensor LM35

3.4 Relay

Relay is a hardware device that is used as an electrical switch. In an electrical circuit the relay is used for a combination of contacts with the conductor like to make contact, break contact or perform a combination of both make and break. A relay works on the principle of electromagnetic induction. It consists of a coil of wire wound about a soft iron core with a mobile armature with single or multiple points of contact with the circuit.

When current passes through the coils by the principle of electromagnetic induction it induces a magnetic flux around the coil that causes the movement of the armature. Depending upon the construction of the circuit and the position of the moveable contacts the circuit connection opens or closes allowing the current to flow or stop respectively. Relays are used whenever we need to control the flow of high current or voltage to a low power device.

Fig 3.4: Relay

4. Existing system

One of the existing method used is a tracer method in which we detect the fault by walking on the cables. Electromagnetic deflections in signals is used to locate the fault point accurately. Another existing method is called the terminal method in which end to end of the cable is testing for open circuit or short circuit. This gives the general overview on the area of fault in the cable. Another less frequently employed method of underground fault detection is called the online method. This uses the sampled voltage and current readings to process the fault points.

5. Proposed system

Our proposed project consist of both hardware and software modules. The major components of the project are a power supply unit, Arduino microcontroller, resistance measurement circuit, manual fault generation switch

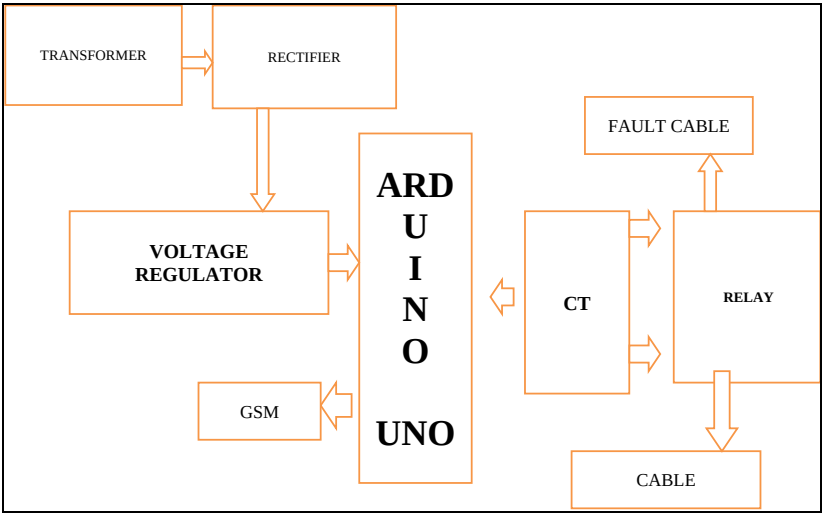

Fig 5: Block Diagram

The power system circuit consist of a step-down transformer which reduces the 230v AC input voltage to 12v AC supply. As the Arduino uses steady direct current as input we send the 12v Alternating current to a rectifier circuit. The 12v alternating current is converted to a 12v direct current in the rectifier. The voltage regulator further reduces the 12v direct current to 5v direct current and also changes the variable current to steady current of 5v. The two types of faults that is generated are due to open circuit and short circuit. The relay is used in the project to make or break the

connection. As the operational supply need for relay is high we use a step-up current transformer is used. For testing purposes, we use a fault generating switch in our proposed model. When a large load current is given as input to current transformer, then output current increases suddenly and the relay detects this change. Due to the sudden increase in the input current there is an induced flux in the relay that makes the relay contacts to move. Now output across the load resistor is passed to the ADC of the Arduino. When a short circuit occurs faults occurring are L-G or L-L and the change in the current is measure across the resistors in the load. The output current difference is then sent to the analog to digital converter of the Arduino. This change in current value is used to compute the distance of the fault location in the cable from the base station. This processed information is sent to GSM module interfaced with the Arduino. The GSM module has a sim and the fault message is sent to the sim connected with the GSM module.

6. Working principle

The major components of the project are a power supply unit, Arduino microcontroller, resistance measurement circuit, manual fault generation switch the power system circuit consist of a step-down transformer which reduces the 230v AC input voltage to 12v AC supply. As the Arduino uses steady direct current as input, we send the 12v Alternating current to a rectifier circuit. The 12v alternating current is converted to a 12v direct current in the rectifier. The voltage regulator further reduces the 12v direct current to 5v direct current and also changes the variable current to steady current of 5v. The two types of faults that is generated are due to open circuit and short circuit. The relay is used in the project to make or break the connection. As the operational supply need for relay is high, we use a step-up current transformer is used. For testing purposes, we use a fault generating switch in our proposed model. When a large load current is given as input to current transformer, then output current increases suddenly and the relay detects this change. Due to the sudden increase in the input current, there is an induced flux in the relay that makes the relay contacts to move. Now output across the load resistor is passed to the ADC of the Arduino. When a short circuit occurs faults occurring are L-G or L-L and the change in the current is measure across the resistors in the load. The output current difference is then sent to the analog to digital converter of the Arduino. This change in current value is used to compute the distance of the fault location in the cable from the base station. This processed information is sent to GSM module interfaced with the Arduino. The GSM module has a sim and the fault message is sent to the sim connected with the GSM module.

7. Results and discussion

The goal is to see whether the fault in the transmission line is detected using our project and the analog to digital converter converts the impedance value across the load and outputs the distance of fault in kilometers. We have successfully tested the device and the fault is measured using the current and the distance of the fault in distance is given by the analog to digital converter and the GSM module sends an error message notification to the user.

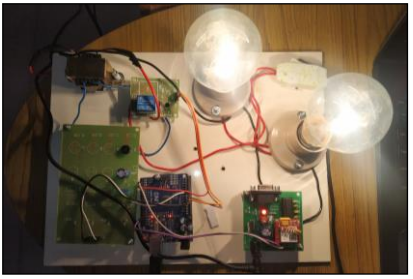

Fig 7: Fault measured output

8. Conclusion

This project has been designed, implemented on an arduino based underground cable fault detector. We have successfully designed, implemented and tested a cheap underground cable fault detector. Our proposed method can detect both open and short circuit in underground cables with an output that gives the distance of the fault from base station in kilometers. Hence the objectives of our project, that is, designing and developing a current driven, portable, highly efficient, low maintenance fault detection system has been designed, developed and tested successfully.

9. Future scope

In this project we detect the exact location of short circuit fault in the underground cable from feeder end in km by using arduino. In future, this project can be implemented to calculate the impedance by using a capacitor in an AC circuit and thus measure the open circuit fault. This project can be used to reduce the man labour involved in fault detection. Also we can reduce the cost involved in correction of the cable faults by many folds. Our project is not limited only to underground cables but can be used on any transmission line to detect fault.

10. References

1. Abhinav Deshpande. Design and implementation of an intelligent security system for farm protection from wild animals, International journal of science and research. 2016; 10(2):300-350.

2. Liu CC, Jung J, Heydt GT, Vittal V, Phadke AG. The Strategic Power Infrastructure Defense (SPID) system. A conceptual design, IEEE Control Syst. Mag. 2000; 20(4):40-52.

3. Filho VX, Pilotto LAS, Martins N, Carvalho ARC, Bianco A. Brazilian defense plan against extreme contingencies, in Proc. IEEE Power Engineering Soc. Summer Meeting. 2001; 2:15-19.

4. Faucon O, Dousset L. Coordinated defense plan protects against transient instabilities, IEEE Comput. Appl. Power. 1997; 10(3):22-26.

5. Trudel G, Bernard S, Scott G. Hydro-Québec's defence plan against extreme contingencies, IEEE Trans. Power Syst. 1999; 14(3):958-965.

6. Jung J, Liu CC. Multi-agent technology for vulnerability assessment and control, in Proc. IEEE Summer Meeting, 2001, 1287-1292.

7. Qiu B, Liu Y, Phadke AG. Communication infrastructure design for Strategic Power Infrastructure Defense (SPID) system, in Proc. IEEE Power Engineering Soc. Winter Meeting. 2002; 1:27-31.

8. Liu Q, Hwang JN, Liu CC. Communication infrastructure for wide area protection of power systems, in Power Systems and Communications Infrastructures for the Future Beijing, China, 2002.

9. You H, Vittal V, Yang Z. Self-healing in power systems: An approach using islanding and rate of frequency decline-based load shedding, IEEE Transactions on Power Systems. 2003; 18:174-181.

10. Cote P, Cote SP, Lacroix M. Programmable load shedding systems Hydro-Quebec's experience, in Proc. IEEE Power Engineering Soc. Summer Meeting. 2001; 2:818-823.

11. Cowbourne DR, Murphy PM. The application of system control centre computer assisted special protection systems in Ontario Hydro, in Proc. 4th Int. Conf. Developments in Power Protection, 1989, 156-161.

12. Anderson PM, LeReverend BK. Industry experience with special protection schemes, IEEE Trans. Power Syst. 1996; 11(3):1166-1179.

13. Denys P, Counan C, Hossenlopp L, Holweck C. Measurement of voltage phase for the French future defence plan against losses of synchronism, IEEE Trans. Power Del. 1992; 7(1):62-69.

14. Lebrevelec C, Cholley P, Quenet JF, Wehenkel L. A statistical analysis of the impact on security of a protection scheme on the French power system, in Proc. Int. Conf. Power System Technology (POWERCON '98). 1998; 2:1102-1106.

15. Elizondo DC, De La Ree J, Phadke AG, Horowitz S. Hidden failures in protection systems and their impact on wide-area disturbances, in Proc. IEEE Power Engineering Soc. Winter Meeting. 2001; 2:710-714.

16. Hsu J, DeShazo G, Wong W. Use of special protection systems to overcome power congestion in the Western United States, in Proc. Int. Conf. Power System Technology (POWERCON '02), 3, 1339-1343.

17. McCalley JD, Fu W. Reliability of special protection systems, IEEE Trans. Power Syst. 1999; 14(4):1400-1406.

18. Fu W, Zhao S, McCalley JD, Vittal V, Abi-Samra N. Risk assessment for special protection systems, IEEE Trans. Power Syst. 2002; 17(1):63-72.

19. Nielsen EK, Coultes ME, Gold DL, Taylor JR, Traynor PJ. An operations view of special protection systems, IEEE Trans. Power Syst. 1988; 3(3):1078-1083.

20. Senders JW. Tampering in nuclear power plant control rooms: Human factors issues, in Conf. Rec. IEEE 4th Conf. Human Factors and Power Plants, 1988, 454-459.

21. Aristizabal M, Cortez S. Transmission line restoration techniques in Colombia, South America, in Proc. 6th Int. Conf. Transmission and Distribution Construction and Live Line Maintenance, 1993, 293-307.

22. Lekkas GP, Avouris NM, Papakonstantinou GK. Development of distributed problem-solving systems for dynamic environments, IEEE Trans. Syst. Man, Cybern. 1995; 5(3):400-414.

Chapter - 4
Transmission System Pricing and Forecasting Methods

Authors

Dr. M. Lakshmikantha Reddy
Associate Professor, EEE, Aditya College of Engineering, Madanapalle, Andhra Pradesh, India

Ch. Narendra Kumar
Associate Professor, EEE, Malla Reddy Engineering College, Secunderabad, Telangana, India

Dr. Y.V. Krishna Reddy
Assistant Professor, Department of EEE, S.V. College of Engineering, JNTUA, Tirupati, Andhra Pradesh, India

Dr. M. Laxmidevi Ramanaiah
Associate Professor, EEE, Institute of Aeronautical Engineering, Hyderabad, Telangana, India

Chapter - 4

Transmission System Pricing and Forecasting Methods

Dr. M. Lakshmikantha Reddy, Ch. Narendra Kumar, Dr. Y.V. Krishna Reddy and Dr. M. Laxmidevi Ramanaiah

Abstract

The power industry across the globe is experiencing a major change in its business as well as in an operational model where, the vertically integrated utilities are being unbundled and opened up for competition with private players putting an end to the era of monopoly. Today energy price forecasting is an important area of research. Market participants of this market such as generators, power suppliers, investors and trades need to maximize their profit. In comparison to load forecasting, electricity price forecasting is much more complicated process. It is because of the distinctive character of electricity which makes it different from other commodities such as its non-storable nature, inelasticity of demand, maintaining a constant balance between demand and supply of power.

Keywords: power demand, transmission pricing, congestion pricing, electricity price voltality, market price and load forecasting

1.1 Introduction

Since early 1980's the electrical industry is going under a continuous change. This change is leading to a complete different atmosphere where the ultimate benefit is provided to the end use customers, with a reliable and cheap electricity supply. This market is a customer driven market and price forecasting is an important tool to the market players. Various models and techniques have been developed by the researchers to determine the correct price in order to obtain the maximum profit. Discussion on various price forecasting techniques and their application in various electricity markets around the world has been discussed here.

1.2 Transmission pricing

Transmission constraints prevent the operation of effective plants. The location of generation that causes the amount of transmission power losses can also be determined by using these constraints. If these conceptions are

neglected by the transmission prices then the system will be ineffective and if it is considered then transmission prices should motivate the construction of new generation or transmission capacity which improves the system efficiency.

Federal Electricity Regulatory Commission (FERC) recognized that transmission grid is the key issue competition and issued guidelines to price of transmission.

The guidelines are summarized such that transmission pricing would

- Meet the traditional requirements of transmission owners.
- Reflect comparability.
- Promote economic efficiency.
- Promotes fairness or credibility.
- Be practical or real time.

Even though transmission costs are small as compared to power production expenses and represent a small percent of major investor-owned utilities, operating expenses, a transmission system is the most important key to competition because it will provide price signals that can create efficiencies in the power generation market.

a) Contract path method

- It has been used between transacted parties of price transmission, where power flows are assumed to flow over a pre-defined path.
- Generally, power flow can take over parallel paths or loop flows owned by several utilities that may not be on the contact path. As a result, transmission owners may not be compensated for the actual use of their facilities. This will results in pancacking i.e. increase in price of the transaction.
- To overcome this pancaking effect, zonal pricing schemes have been proposed. Here the ISO zonal transmission system is divided into zones and a transmission user will rates based on energy prices in zones, where power is injected or withdrawn.

b) MW-Mile Approach/Method

- The MW-Mile rate is basically based on the distance between transacted parties and flow in each line resulted from the transaction. This approach takes into account parallel flows and eliminates previous problem that transmission owners were not compensated for using their facilities.

- This method is complicated because every change in transmission line or transmission equipment requires re-calculation of flows & charges in lines.

The charges for each transaction are calculated as below.

$$C_{mn,j} = \frac{(f_{mn,j})(D_{mn})(R_{mn})}{f_{mn}}$$

$$C_{mn,j} = \frac{f_{mn,j}}{f_{mn}} Z_{mn}$$

Where,

$C_{mn,j}$ → Total charge for transaction while loading line m–n during j^{th}.

$f_{mn,j}$ → Loading of the line m-n during j^{th} transaction.

D_{mn} → Distance of the line m-n (in miles).

R_{mn} → Revenue per unit length (Rs./mile).

and Total Revenue on line m-n is $Z_{mn} = D_{mn} R_{mn}$.

1.3 Congestion pricing

The over load condition is occur in a transmission lines or transformers is called as "Congestion". Congestion prevents system operators from dispatching additional power from a specific generator. Congestion would be caused for various reasons such as transmission line outages, generator outages, change in energy demand and un-coordinated transactions.

The congestion can be controlled by

- Means of reservations rights and congestion pricing.
- Applying controls like phase shifters, tap changing transformers, reactive power control, re- scheduling of generation and load limitation.

Congestion pricing methods

By employing all new restructuring schemes are considering congestion costs into account in order to calculate congestion costs and assign these costs to the users of transmission systems. Based on the following three methods these approaches are developed as follows.

a) Costs of out-of-merit dispatch

This is suitable to systems with less significant transmission congestion problems. In this approach, congestion costs are allocated to each users of transmission system based on ratio of load sharing.

b) Locational marginal prices (LMP)

- This technique depends on the cost of supplying energy to the next increment of load at a particular location on the transmission grid.
- It evaluates the price paid for the energy by buyers in a competitive market at particular locations and by observing the variation in LMP's between two locations congestion costs are measured, in this approach based on the bid's supplied to the power exchange (PX).
- The LMP's are calculated at all nodes of transmission system based on bids provided in PX.

c) Usage charges of inter-zonal lines

In this approach, the ISO region is classified into congestion zones based on the historical performance. Violations of transmission lines between zones (inter-zonal lines) are severe, while the transmission constraints are small in congestion zone. All transmission users pay usage charges for using the inter-zonal lines. In order to increase or decrease power generation the usage charges will be calculated from bids submitted by the market participants.

Adjustment bids indicate a participants willingness to adjust power generation at a particular cost.

Ex: California model

1.4 Management of inter-zonal/intra-zonal congestion

Transmission network plays a major role in the open access restructured power market. It is perceived phase shifters and tap-transformers plays vital role and corrective actions in congestion management without re-dispatch. In this type of market, transmission congestion problems could be handled more easily when inter-zonal/ intra-zonal scheme is implemented.

A congestion problem formulation should take into consideration interactions between intra zonal and inter zonal flows and their effects on the power system.

Inter-Zonal Congestion	Intra-Zonal Congestion
1. The congestion which primarily occurs on transmission interfaces	1. The congestion which occurs within a congestion zone due to network

between congestion zones is known as "Inter-Zonal Congestion"	constraints in it known as "Intra-Zonal Congestion"
2. It is frequent and expensive with wide spread effects.	2. It is infrequent and inexpensive with the localized effects
3. Its objective to improve reliability and efficiency.	3. Its objective is to improve reliability and hold maximum customer choices.
4. Scheduling Coordinators (SC's) are changed or paid externally for using the inter-zonal interface depending upon the direction.	4. Scheduling coordinators (SC's) are not changed externally for using the intra-zonal interface.
5. In this congestion, SC's are charged and paid if the interface is used in the same and opposite directions respectively.	5. In this, congestion is independent of the interface used by the SC's.
6. Participating transmission owners (PTO's) receive congestion revenues, which effect on the next year's access fees.	6. PTO's does not receive congestion revenues and has no effect on the next year's access fees
7. Different MCPs are paid by supply resources due to their location in different zones. Usually the supply paid is less in from-zone and more in to-zone	7. Same MCP is paid by supply resources irrespective of their specific location in the zone.
8. Different MCPs are paid by demand resources due to their location in different zones. Usually the demand pays less in from-zone and more in to-zone	8. Same MCP is paid by the demand resources irrespective of their specific location in the zone.
9. **Control varibles** a) SC's power generation in all congestion zones. b) SC's adjustable loads. c) For each load, a set of load quantities with adjustment for decremented bids are submitted by SC.	9. **Control Varibles** a) SC's power generation in congestion zone only. b) SC's adjustable loads in the congestion zone. c) Reactive power controls including bus voltages, reactive power injection, tap-transformers.
10. **Constraints** a) Limits on control variables. b) Nodal active power flow balance equations. c) Inter-zonal line flow inequality constraints. d) Market separation between SCs.	10. **Constraints** a) Limits on control variables b) Nodal active & reactive power flow balance equations c) Intra-zonal MW and MVAr line flows inequality constraints d) Voltage Limits, e) Stability Limits, f) Contingency Limits

1.5 Electric price volatility

Volatility is the most distinct property of electricity. Electricity price volatility is a measure of instability in future prices or uncertainty in the future price movements in a specific period of time. It is usually represented by as a percentage and evaluated as authorized standard deviation of daily price percentage change. Volatility in electricity market is used to examine various hedging strategies and portfolios. It depends on time and may reflect the value of electricity derivatives like options and future.

When spot price is highly volative, the value of the energy option would be high. The load and price curves for the Pennsylvania -New Jersey Model (PJM) power market from 1/1/99 to 1/14/99 are shown in following Fig 5.3 and Fig 5.4 respectively.

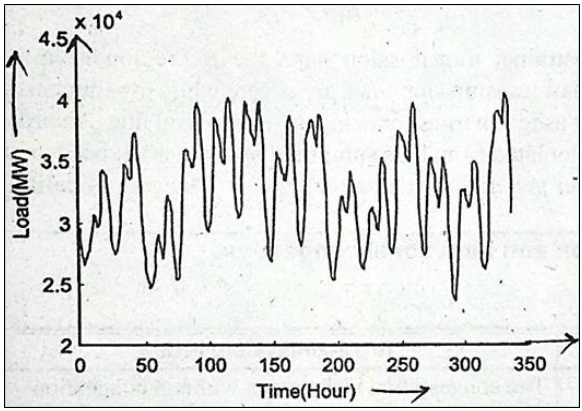

Fig 5.3: Load curve of PJM Power Market

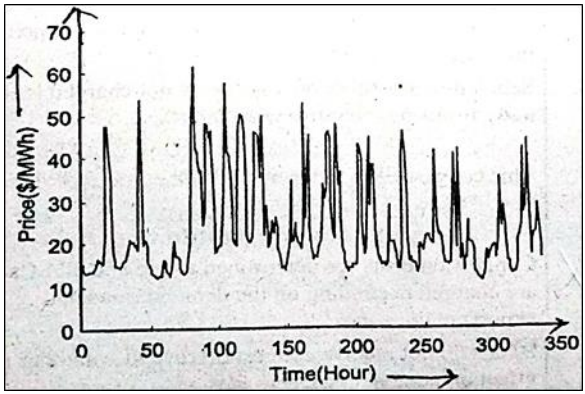

Fig 5.4: Price Curve of PJM Power Market

From the curves, we can observe that:

- The load curve is comparatively homogeneous and its variations show a cyclic property.
- The price curve is a non-homogeneous and its variations exhibits less cycle property.
- Practicing market power by dominant generators could cause volatility in addition to raising prices over competitive levels.
- Load forecasting error is an important factor in price volatility in price more is more severe.
- The reason for spikes is due to the forced outages of power system components.
- Volatility is also depends on supply, demand and unexpected outages.

The basic reason behind the electricity price volatility is to match supply and demand on time basis.

The other reasons are:

1) Volatility in fuel price.
2) Uncertainty in load.
3) Uncertanty in generation outages.
4) Alternators in hydro electricity production.
5) Transmission congestion.
6) Market participants behaviour based on expected price.
7) Market operation based on market price and risk.

Due to the special features of electricity, the electricity price is more volatile compared to non-energy commodities.

According to the study released in 1997, the WIT oil future contracts annualized volatility is about 28%. Due to the volatility factors, precise forecast for the electricity spot market is complicated to be determined. Hence, it is clear that the accuracy of existing price forecasting is much lower than that of the load forecasting. According to the year 2001, the least price forecasting error was about 10% as compared to load forecasting error of about 3%. However, the accuracy of price forecasting is not severe as load forecasting.

1.6 Challenges to electricity pricing

The challenges faced on pricing in electricity market are as follows.

1) Pricing Model.
2) Reliable forward curves.

1. Pricing model

Selecting the most suitable pricing strategy is a major task in markets. Traditionally, 'Block- scholes model' is one of the important pricing models, which is used to provide pricing to the physical power options. The use of this version leads to a major problem by the market participants (i.e. market hedges) in restructured market of electricity.

Block-scholes model was originated as the pricing model to provide monetary worth to European securities and future options. The theory is based on certain assumptions that the pricevolatile condition is constant, price series is continuous and the nature of electricity is also considered which is different from other goods. As per this model, the price dynamics are given by

$$\left| \frac{dF(t,T)}{F(t,T)} = b\,dW(t) \right|$$

Where,

F (t,T) $\rightarrow$ price at time 't ' for future delivery of power at time T.

b $\rightarrow$ Constant of Volatility.

dW (t) $\rightarrow$ Standard Brownian motion.

2. Reliable forward curves

A curve represents a set of forward or future prices for electricity is known as forward price curve. (or) A curve which shows the variation of future prices with time is known as forward price curve. A set of present market prices are determined by this curve for the electricity sale at specified times in the future. It determines the current value of electricity to be transported in future.

In electricity market, forward curve is a measure or index value. The increase in future prices in the curve increases present values of production services and purchase contracts. Similarly, decline in forward curve represents decrease in the value of existing sales contracts and a utility's consumer base.

1.7 Construction of forward price curves

The construction of forward price curves mainly depends on

1) Time frame for price curves.
2) Types of forward price curves.

1. Time frame for price curves

The construction of forward price curves mainly depends on a time frame, which may be for

i) Short-Term (for Few Months).
ii) Medium-Term (for Few Years).
iii) Long-Term (for Several Years).

The price of electricity mainly changes with respect to changes in weather conditions, supply outages, wind conditions, inter-regional power flow etc.

2. Types of forward price curves

The forward electricity price plays a key role for pricing retail and wholesale electricity. Forward curves represent good starting criterion to price electricity and characteristics and supply or demand situations.

The construction of reliable forward price curves and volatility forecast for a particular period of time is based on the supply and demand balanced analysis in the electricity market and by considering the fluctuations in the fuel costs and load.

The forward curve includes three behaviours. They are

A) Backwardation
B) Contango
C) Combination of both

A) Backwardation

It is a market condition in which the spot prices are exceeds the future prices. It is also known as inverted market. It gives the relationship between forward and spot market in which the shorted-dated contracts deals with higher price and the longer dated contracts (future market) deals market with lower price.

In order to attract the buyers for trading with sellers, it is essential to keep the forward price lower than the expected spot price. The representation of backwardation is shown in Fig. 5.5 by plotting the change in price with time.

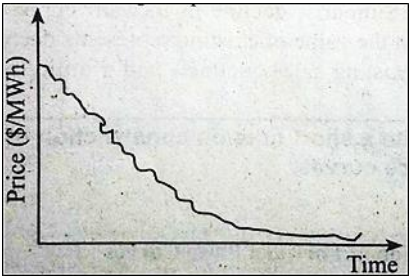

Fig 5.5: Backwardation

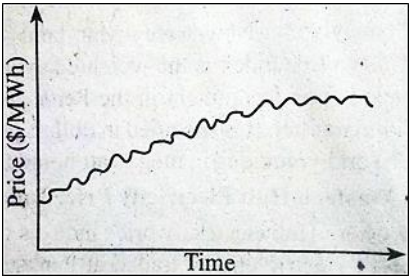

Fig 5.6: Contango

B) Contango

Contango is opposite to the backwardation. It is always used to mention electricity markets, where the short-dated deals with lower than the longer-dated contracts in future contracts. The contango curve shows the slope upwards as shown in above Fig. 5.6.

Contango gives a forward or spot market relationship in which the forward price exceeds the spot price. Usually, the forward price is more than the spot price by approximately the net cost carry or finance the spot electricity or security until the forward contract settlement date.

C) Combination of both

The combination of backwardation and contango is shown in Fig 5.7. This is an example of a condition in which the forward curve takes form of backwardation in the short-term part of the curve and in the long-term part of the curve. It is a combination of two. The curve behaviour on expectations with respect to power supply (or) load demand balance in the market besides the other seasonal factors that manage prices.

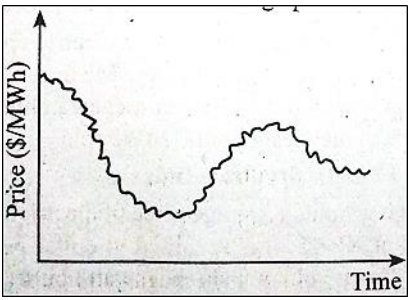

Fig 5.7: Combination of Backwardation and Contango

Short-time price forecasting

There are many physical factors that will impact short-term electricity price. In practice, it is not possible to include all the factors in price

forecasting, because all factors are unknown or the related data is not available.

The change in the price movement gives a conceptual understanding of factors impacting electrical price. The movements in a price are analyzed by the variations in spot price or market clearing price (MCP). MCP is the intersection of supply and demand curve as shown in figure.

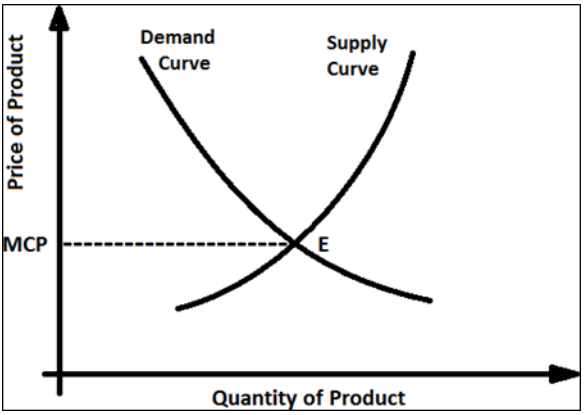

Fig 5.6: Calculation of Market Clearing Price (MCP)

The curve attains equilibrium at 'E', where the supply and demand curve meet in the short-term forecasting.

1.8 Forecasting methods

1) Simulation method.
2) Artificial Neural Network method.
3) Analysing Foresting Errors.

1. Simulation method

- Usually, the analysis of price volatility is based on the probability distribution for each of a series of key drivers. The users can determine the distribution of input variables using historical data.
- To capture the effects of uncertainty, samples are drawn from the distribution of the input variable using monte-carlo methods and a scenario is created. For each scenario the tool is used to simulate the market prices.
- The volatility indices and all the traditional measures are then developed from the statistical distribution of the variables.

2. Artificial neural network method

The artificial neural network method has received more attention in the field of forecasting because it is clear model, easy implementation and good performance.

This method was applied before to load forecasting in electric power systems. Here, we use the MATLAB for training the artificial neural network in the short-term price forecasting, which provides a very powerful tool for analyzing factors that could impact clearing prices.

3. Analysing forecasting errors

There are three types of forecasting errors. They are

A) Percentage Error (PE).

B) Absolute Percentage Error (APE).

C) Mean Absolute Percentage Error (MAPE).

A. Percentage Error (PE)

The percentage error is defined as the ratio of difference between the forecasted value and actual value to the actual value. It is a relative error represented in terms of percentage.

Let V_a nad V_f the actual and forecasting value and actual values respectively. Then the Percentage Error (PE) is calculated as

$$PE = \left(\frac{\text{Forecasting value - Actual value}}{\text{Actual value}} \right) * 100$$

$$\therefore PE = \left(\frac{V_f - V_a}{V_a} \right) * 100$$

B. Absolute Percentage Error (APE)

The magnitude of Percentage Error (PE) is referred as Absolute Percentage Error (APE) mathematically, it is expressed as,

$$APE = |PE|$$

$$\therefore APE = \left| \left(\frac{V_f - V_a}{V_a} \right) * 100 \right|$$

When actual values are more than the forecast value then APE will be nearly 100%. In future, if actual value is small, then the small difference between forecasted and actual values causes very large APE.

For instance, if the actual value is zero, then APE will be infinity for non-zero forecasted value. So, APE is difficult for price forecasting. It should be observed that such problems will occur in load forecasting because price is very small or zero and actual values are quite large.

C. Mean Absolute Percentage Error (MAPE)

The prediction accuracy measurement of a forecasting method in statistics is called as mean Absolute Percentage Error (MAPE). It is also known as MAPD (mean Absolute Percentage Deviation).

MAPE is also defined as the percentage of mean average of the error i.e. the difference between the forecasted value and actual value divided by the actual value and the mean of which can be expressed in terms of percentage. Mathematically it is expressed as,

$$MAPE = \frac{1}{N}\sum_{i=1}^{N}\left|\left(\frac{V_f - V_a}{V_a}\right)*100\right|$$

$$MAPE=\frac{1}{N}\sum_{i=1}^{N} APE_i$$

It is widely used to determine the load forecasting performance. However, in price forecasting, MAPE is not a suitable criterion as it may give inaccurate representation. Since if actual value is large, the forecasted value is small, APE will be very large if the difference between the actual and forecasted value is small. Hence, we define the average value.

$$i.e.\ V = \frac{1}{N}\sum_{i=1}^{N} V_a$$

$$\left(\frac{V_f - V_a}{V_a}\right)$$

$$APE=|PE|$$

$$MAPE=\frac{1}{N}\sum_{i=1}^{N} APE_i$$

1.9 Conclusion

This chapter is about electricity market price forecasting techniques and their application in various markets. For profit maximization forecasting is but forecasting of price forecasting is a complicated because of the distinguishing features of price as discussed above. Every electricity market is different type

therefore, there is no general method for price forecasting it can vary as per market requirements. Different forecasting methods, such as models, are reviewed separately along with different markets they are used in. The future trend is using of Hybrid methods which combine different models to compensate the weakness of individually established models increasing the performance characteristics of these models by reducing forecasting errors.

References

1. Aggarwal SK, Saini LM, Kumar A. Electricity Price Forecasting in Deregulated Markets: A Review and Evaluation. International Journal of Electrical Power & Energy Systems. 2009; 31:13-22.
2. Niimura T. Forecasting Techniques for Deregulated Electricity Market Prices-Extended Survey. IEEE PES Power Systems Conference and Exposition, Atlanta, 2006, 51-56.
3. Bunn DW. Forecasting loads and prices in competitive power markets. Proc IEEE. 2000; 88(2):163-9.
4. Xian Zhang, Xifan Wang. Overview on Short-term Electricity Price Forecasting, Automation of Electric Power Systems, 2006, 30(3).
5. Nitin Singh, Mohanty SR. A Review of Price Forecasting Problem and Techniques in Deregulate Electricity Markets Journal of Power and Energy Engineering. 2015; 3:1-19.
6. Hu L, Taylor G, Wan HB, Irving M. A Review of Short-Term Electricity Price Forecasting Techniques in Deregulated Electricity Markets. Universities Power Engineering Conference (UPEC), Proceedings of the 44th International, Glasgow, 2009, 1-5.
7. Niimura T. Forecasting Techniques for Deregulated Electricity Market Prices, IEEE Power Engineering Society General Meeting, 2006.
8. Sudhakara Reddy AV, Ramasekhara Reddy M, Vijaya Kumar M. Stability Improvement During Damping of Low Frequency Oscillations with Fuzzy Logic Controller, International Journal of Engineering Research and Applications (IJERA). 2012; 2(5):1560-1565.
9. Bhargava Reddy B, Sivakrishna D, Sudhakara Reddy AV. Modelling and Analysis of Wind Power Generation Using PID Controller, International Journal for Scientific Research & Development (IJSRD). 2013; 1(9):2045-2049.
10. Prasad P, Bhargava Reddy B, Sudhakara Reddy AV. Power Loss Minimization in Distribution System using Network Reconfiguration

with Particle Swarm Optimization, International Journal of Engineering Science & Advanced Technology (IJESAT). 2015; 5(3):171-178.

11. Surekha K, Sudhakara Reddy AV. A New Control Topology for Smart Power Grids using Bi-directional Synchronous VSC, International Journal of Informative & Futuristic Research. 2015; 2(10):3695-3704.
12. Sudhakara Reddy AV, Damodar Reddy M, Vinoda N. Optimal Placement of Dynamic Voltage Restorer in Distribution Systems for Voltage Improvement using Particle Swarm Optimization, International Journal of Engineering Research and Applications (IJERA). 2017; 7(3):29-33. ISSN: 2248-9622.
13. Sudhakara Reddy AV, Damodar Reddy M. Optimization of Distribution Network Reconfiguration using Dragonfly Algorithm, Journal of Electrical Engineering. 2017; 16(4-30):273-282. ISSN:1582-1594.
14. Bharathi S, Sudhakara Reddy AV, Damodar Reddy M. Optimal Placement of UPFC and SVC using Moth-Flame Optimization Algorithm, International Journal of Soft Computing and Artificial Intelligence. 2017; 5(1):41-45.
15. Sudhakara Reddy AV, Damodar Reddy M. Optimal Capacitor allocation for the reconfigured Network using Ant Lion Optimization algorithm, International Journal of Applied Engineering Research (IJAER). 2017; 12(12):3084-3089.
16. Sudhakara Reddy AV, Damodar Reddy M. Network Reconfiguration of Distribution System for maximum loss reduction using Sine Cosine Algorithm, International Journal of Engineering Research and Applications (IJERA). 2017; 7(10):34-39.
17. Sudhakara Reddy AV, Damodar Reddy M, Satish Kumar Reddy M. Network Reconfiguration of Distribution Systems for Loss Reduction using GWO algorithm, International Journal of Electrical and Computer Engineering (IJECE). 2017; 7(6):3226-3234.
18. Sudhakara Reddy AV, Damodar Reddy M. Distribution Network Reconfiguration for Maximum Loss Reduction using Moth Flame Optimization, International Journal of Emerging Technologies in Engineering Research (IJETER). 2018; 6(1):86-90.
19. Sudhakara Reddy AV, Dr. M Damodar Reddy. Application of Whale Optimization Algorithm for Distribution Feeder Reconfiguration, i-manager's Journal on Electrical Engineering. 2018; 11(3):17-24.

20. Sudhakara Reddy AV, Damodar Reddy M, Krishna Reddy YV. Feeder Reconfiguration of Distribution Systems for Loss Reduction and Emissions Reduction using MVO Algorithm, Majlesi Journal of Electrical Engineering. 2018; 12(2):1-8.

21. Kalyani S, Sudhakara Reddy AV, Vara Prasad N. Optimal Placement of Capacitors in Distribution Systems for Emission Reduction using Ant Lion Optimization Algorithm, International Journal of Current Advanced Research. 2018; 7(11):16339-16343.

22. Sudip Sardar, Mr. P Kamalakar, Mr. Sudhakara Reddy AV, Dr. Ezhil Vignesh K. Car Parking Monitoring System using Lab View, Journal of Research in Science, Technology, Engineering and Management (JoRSTEM). 2019; 5(1):66-72.

23. Sudhakara Reddy AV, Praveen Kumar Reddy Y, Bhargava Reddy B, Krishna Reddy YV. Application of ALO to Economic Load Dispatch Without Network Losses for Different Conditions, 2nd IEEE International Conference on Power Electronics, Intelligent Control and Energy Systems (ICPEICES), New Delhi, India, 2018, 244-248.

24. Ram Shankar Singh, Naveen Venkat V, Mr. Sudhakara Reddy AV, Dr. Raja Reddy D. IOT Home Automation via Google Assistance, Journal of Research in Science, Technology, Engineering and Management (JoRSTEM). 2019; 5(1):44-53.

25. Priyanka G, Prudhvi Raj M, Mr. Ramesh D, Mr. Sudhakara Reddy AV. Human Safety Device using GSM and GPS Module, Journal of Research in Science, Technology, Engineering and Management (JoRSTEM). 2019; 5(1):83-88.

26. Manogna Reddy V, Dr. Raja Reddy D, Mrs. Sudha Reddy Y, Mr. Sudhakara Reddy AV. Effective Load Sharing of Distribution Transformer using GSM, Journal of Research in Science, Technology, Engineering and Management (JoRSTEM). 2019; 5(1):73-77.

27. Krishna Reddy YV, Damodar Reddy M, Sudhakara Reddy AV. Flower Pollination Algorithm for Solving Economic Dispatch with Prohibited Operating Zones and Ramp Rate Limit Constraints, Journal of Emerging Technologies and Innovative Research (JETIR). 2018; 5(10):498-505.

28. Sudhakara Reddy AV, Rajeswaran N, Raja Reddy D. Application of modified ALO to economic load dispatch for coal fired stations, International Journal of Recent Technology and Engineering (IJRTE). 2019; 8(2):2147-2152.

29. Jhansi Reddy, Nikitha Reddy, Raja Reddy D, Dr. Sudhakara Reddy AV. Smart Traffic Control System using Sensors, International Journal of Research and Advanced Development (IJRAD). 2019; 3(3):14-16. ISSN: 2581-4451

30. Krishna Reddy YV, Damodar Reddy M, Sudhakara Reddy AV. Flower Pollination Algorithm to Solve Dynamic Economic Loading of Units with Practical Constraints, International Journal of Recent Technology and Engineering (IJRTE). 2019; 8(3):535-542.

31. Sudhakara Reddy AV, Prof. M Damodar Reddy. Optimization of network reconfiguration by using particle swarm optimization, IEEE First International Conference on Power Electronics, Intelligent Control and Energy Systems (IEEE ICPEICES), Delhi Technological University (DTU), New Delhi, India, 2016, 1-6.

32. Sabarinath G, Gowri Manohar T, Sudhakara Reddy AV. Voltage Control and Power Loss Reduction in Distribution Networks using Distributed Generation, International Journal of Innovative Technology and Exploring Engineering (IJITEE). 2019; 8(12):2863-2867.

33. Praveen Kumar Reddy Y, Vara Prasad N, Sudhakara Reddy AV. A Power Sensor Tag with Interference Reduction for Electricity Monitoring of Two-Wire Household Appliances, Journal of Research in Science, Technology, Engineering and Management (JoRSTEM). 2020; 6(1):31-35.

34. Bhargava Reddy B, Nagarjuna P, Sudhakara Reddy AV. Traffic Signal Control using Lab View, Journal of Research in Science, Technology, Engineering and Management (JoRSTEM). 2020; 6(1):1-4.

35. Sudhakara Reddy AV, Laxmidevi Ramanaiah M, Krishna Reddy YV, Navya B, Hari Krishna K, Mahender A. Feeder Protection From Over Load Situations through IoT, International Journal of Future Generation Communication and Networking. 2020; 13(3):3699-3707. ISSN: 2233-7857.

36. Raja Reddy D, Anitha Reddy K, Narendra Kumar Ch, Siva Sai Rama Krishna R, Sudhakara Reddy AV, Rajesh Reddy Duvvuru. Design of Transformer Less UPFC based on Multilevel Inverter, International Journal of Electrical Engineering and Technology (IJEET), 2020, 11(4).

37. Ch. Narendra Kumar, Rajesh Reddy D, Raja Reddy D, Sudhakara Reddy AV, Manoz Kumar Reddy K. Histogram Pattern and Kalman Filter Approach Based Real Time Object Recognition and Tracking System Journal of Critical Reviews. 2020; 7(6):1282-1289.

38. Sudhakara Reddy AV, Md. Imran Ahmed, Ch. Rami Reddy, Ch. Narendra Kumar. Power Quality Improvement in Integrated System using Inductive UPQC, International Journal of Renewable Energy Research (IJRER), 2021.

Chapter - 5
Introduction to Phasor Measurement units in Power Systems

Authors

Dr. Rekharani Maddula
Assistant Professor in Physics, Sri Indu College of Engineering and Technology, Ranga Reddy, Telangana, India

Kesava Vamsi Krishna V.
Associate Professor in Physics, Malla Reddy Engineering College, Secunderabad, Telangana, India

Chapter - 5

Introduction to Phasor Measurement units in Power Systems

Dr. Rekharani Maddula and Kesava Vamsi Krishna V.

Abstract

A phasor measurement unit (PMU) is a device used to estimate the magnitude and phase angle of an electrical phasor quantity such as voltage or current in the electricity grid using a common time source for synchronization. Time synchronization is usually provided by GPS or IEEE 1588 Precision Time Protocol, which allows synchronized real-time measurements of multiple remote points on the grid. PMUs can also be used to measure the frequency in the power grid. A typical commercial PMU can report measurements with very high temporal resolution, up to 120 measurements per second. This helps engineers in analyzing dynamic events in the grid which is not possible with traditional SCADA measurements that generate one measurement every 2 or 4 seconds. Therefore, PMUs equip utilities with enhanced monitoring and control capabilities and are considered to be one of the most important measuring devices in the future of power systems.

Keywords: SCADA, grid, voltage, current, synchronization, frequency

1.1 Phasor Measurement Unit (PMU)

A Synchrophasor is a phasor that is time stamped to an extremely precise and accurate time reference. ´Basically a solid-state relay or digital fault recorder with GPS clock. Synchronized phasors (synchrophasors) provide a real-time measurement of electrical quantities across the power system. The resultant time tagged phasors can be transmitted to a local or remote receiver at rates up to 60 samples per second. Continuously measures voltages and current phasors and other key parameters and transmits time stamped messages.

PMUs are capable of capturing samples from a waveform in quick succession and reconstructing the phasor quantity, made up of an angle measurement and a magnitude measurement. The resulting measurement is

known as a synchrophasor. These time synchronized measurements are important because if the grid's supply and demand are not perfectly matched, frequency imbalances can cause stress on the grid, which is a potential cause for power outages [1]. A typical commercial PMU can report measurements with very high temporal resolution, up to 120 measurements per second. This helps engineers in analyzing dynamic events in the grid which is not possible with traditional SCADA measurements that generate one measurement every 2 or 4 seconds. Therefore, PMUs equip utilities with enhanced monitoring and control capabilities and are considered to be one of the most important measuring devices in the future of power systems [2]. A PMU can be a dedicated device, or the PMU function can be incorporated into a protective relay or other device. he following illustrates information provided by two PMUs on opposite sides of a transmission line:

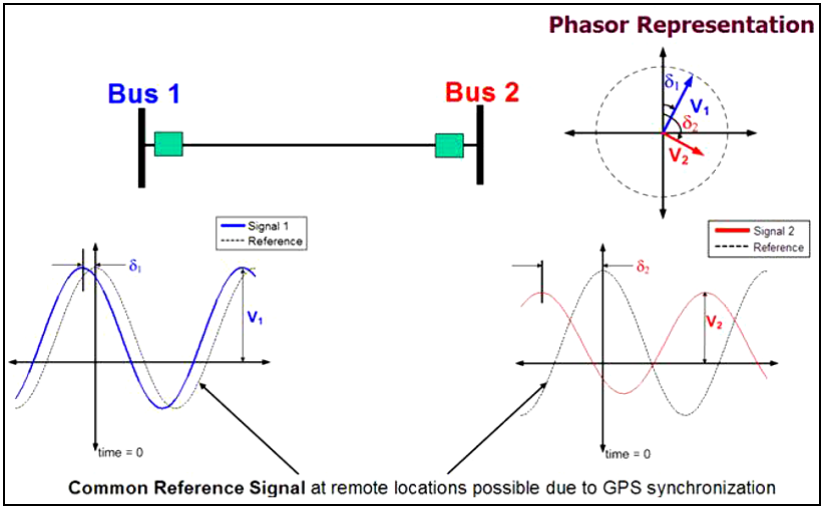

Fig 5.1: Consortium for Electric Reliability Technology Solutions

In 1893, Charles Proteus Steinmetz presented a paper on simplified mathematical description of the waveforms of alternating current electricity. Steinmetz called his representation a phasor [4]. With the invention of phasor measurement units (PMU) in 1988 by Dr. Arun G. Phadke and Dr. James S. Thorp at Virginia Tech, Steinmetz's technique of phasor calculation evolved into the calculation of real time phasor measurements that are synchronized to an absolute time reference provided by the Global Positioning System. We therefore refer to synchronized phasor measurements as synchrophasors. Early prototypes of the PMU were built at Virginia Tech and Macrodyne [5] built the first PMU (model 1690) in 1992 [6]. Today they are available commercially.

With the increasing growth of distributed energy resources on the power grid, more observability and control systems will be needed to accurately monitor power flow. Historically, power has been delivered in a unidirectional fashion through passive components to customers, but now that customers can generate their own power with technologies such as solar PV, this is changing into a bidirectional system for distribution systems. With this change it is imperative that transmission and distribution networks are continuously being observed through advanced sensor technology, such as-PMUs and uPMUs.

In simple terms, the public electric grid that a power company operates was originally designed to take power from a single source: the operating company's generators and power plants, and feed it into the grid, where the customers consume the power. Now, some customers are operating power generating devices (solar panels, wind turbines, etc.) and to save costs (or to generate income) are also feeding power back into the grid. Depending on the region, feeding power back into the grid may be done through net metering. Because of this process, voltage and current must be measured and regulated in order to ensure the power going into the grid is of the quality and standard that customer equipment expects (as seen through metrics such as frequency, phase synchronicity, and voltage). If this is not done, as Rob Landley puts it, "people's light bulbs start exploding [7]. This measurement function is what these devices do.

1.2 Motivation

- Need for more electricity.
- Integration and management of renewable energy.
- Optimal use of ageing assets.
- Ensure reliability of supply.
- Energy efficiency and security.
- Dynamic operation of power system.

1.3 Power system operational paradigm

- Sense
- Communicate
- Compute
- Visualize
- Control
- Situational Awareness and Decision Support.

Phasor data concentrator

Aligns information by time the incoming PMU messages from multiple measuring devices and sends out the aggregated synchronized data set as a single data stream. 'Archive data and process the information'. Exchange records with PDCs at other locations.

Communication

Links multiple PMUs to a PDC (or PDCs to other PDCs) for real time data transfer.

Secure VPN connection from a communications center.

1.4 Phasor measurement unit-measurements

PMUs measure (synchronously):

- Positive sequence voltages and currents.
- Phase voltages and currents.
- Local frequency.
- Local rate of change of frequency.
- Circuit breaker and switch status.

1.5 Real time dynamics monitoring system (RTDMS)

RTDMS is a Synchro-phasor software application for providing real time, wide area situational awareness to Operators, Reliability Coordinators, Planners and Operating Engineers, as well as the capability to monitor and analyze the dynamics of the power system.

RTDMS provides critical metrics of grid dynamics, like

- Phase Angle Differences (Grid Stress).
- Small Signal Stability (Oscillations & Damping).
- Frequency Instability.
- Generation-Load Imbalance.
- Power-Angle Sensitivity.
- Power-Voltage Sensitivity.

1.6 Applications

PMUs provide a detailed and accurate view of power quality across a wide geographic grid. The data collected tells the system operator if the voltage, current and frequency is staying within specified tolerances. The capability is used in multiple ways:

- To improve the accuracy of modeling system conditions.
- To predict and detect stress and instability on the grid.
- To provide information for event analysis after a disturbance has occurred.
- To identify inefficiencies.
- To predict and manage line congestion.

1.7 Conclusion

In recent years, tens of thousands of PMUs have been installed in transmission grids throughout the world. In some cases they are also used in distribution grids. Coupled with smart controllers, PMU offer the opportunity to replace typical hands-on adjustments required by SCADA systems with a system that makes decisions and sends control signals autonomously. Such capabilities promise to allow for more robust and efficient integration of renewables, distributed energy resources (DERs), and microgrids. PMUs are becoming a key tool in making our grid more reliable, resilient and ultimately cleaner.

References

1. De Boer R. Technologies and Prospects for Photochemical Conversion and Storage of Solar Energy: A survey of the state-of-threat, ed., ECN-C--01-029, 2001, 7-9.
2. Baird C. Environmental Chemistry, 2nd ed., W.H. Freeman and Company, NY, 1999, 251-251.
3. www.google.com
4. Chopra KL. Thin Film Phenomena, (McGraw Hill, New York), 1969.
5. Gao Y, Niu H, Chen CQ. Chem. Phys. Lett. 2003; 367(1-2):141.
6. Brown MP, Austin K. The New Physique (Publisher Name, Publisher City), 2005, 25-30.
7. Wang RT. “Title of Chapter”, in Classic Physiques, edited by Hamil RB (Publisher Name, Publisher City), 1999, 212-213.
8. Brown MP, Austin K. Appl. Phys. Letters. 2004; 85:2503-2504.
9. Improvement of reactor efficiency by steam entrainment. International Journal of Hydrogen Energy, 25, 739-745.
10. Sudhakara Reddy AV, Ramasekhara Reddy M, Vijaya Kumar M. Stability Improvement During Damping of Low Frequency Oscillations

with Fuzzy Logic Controller, International Journal of Engineering Research and Applications (IJERA). 2012; 2(5):1560-1565.

11. Bhargava Reddy B, Sivakrishna D, Sudhakara Reddy AV. Modelling and Analysis of Wind Power Generation Using PID Controller, International Journal for Scientific Research & Development (IJSRD). 2013; 1(9):2045-2049.
12. Prasad P, Bhargava Reddy B, Sudhakara Reddy AV. Power Loss Minimization in Distribution System using Network Reconfiguration with Particle Swarm Optimization, International Journal of Engineering Science & Advanced Technology (IJESAT). 2015; 5(3):171-178.
13. Surekha K, Sudhakara Reddy AV. A New Control Topology for Smart Power Grids using Bi-directional Synchronous VSC, International Journal of Informative & Futuristic Research. 2015; 2(10):3695-3704.
14. Sudhakara Reddy AV, Damodar Reddy M, Vinoda N. Optimal Placement of Dynamic Voltage Restorer in Distribution Systems for Voltage Improvement using Particle Swarm Optimization, International Journal of Engineering Research and Applications (IJERA). 2017; 7(3):29-33. ISSN: 2248-9622.
15. Sudhakara Reddy AV, Damodar Reddy M. Optimization of Distribution Network Reconfiguration Using Dragonfly Algorithm, Journal of Electrical Engineering. 2017; 16(4-30):273-282. ISSN: 1582-1594.
16. Bharathi S, Sudhakara Reddy AV, Damodar Reddy M. Optimal Placement of UPFC and SVC using Moth-Flame Optimization Algorithm, International Journal of Soft Computing and Artificial Intelligence. 2017; 5(1):41-45.
17. Sudhakara Reddy AV, Damodar Reddy M. Optimal Capacitor allocation for the reconfigured Network using Ant Lion Optimization algorithm, International Journal of Applied Engineering Research (IJAER). 2017; 12(12):3084-3089.
18. Sudhakara Reddy AV, Damodar Reddy M. Network Reconfiguration of Distribution System for maximum loss reduction using Sine Cosine Algorithm, International Journal of Engineering Research and Applications (IJERA). 2017; 7(10):34-39.
19. Sudhakara Reddy AV, Damodar Reddy M, Satish Kumar M. Reddy "Network Reconfiguration of Distribution Systems for Loss Reduction using GWO algorithm, International Journal of Electrical and Computer Engineering (IJECE). 2017; 7(6):3226-3234.

20. Sudhakara Reddy AV, Damodar Reddy M. Distribution Network Reconfiguration for Maximum Loss Reduction using Moth Flame Optimization, International Journal of Emerging Technologies in Engineering Research (IJETER). 2018; 6(1):86-90.
21. Sudhakara Reddy AV, Dr. M Damodar Reddy. Application of Whale Optimization Algorithm for Distribution Feeder Reconfiguration, i-manager's Journal on Electrical Engineering. 2018; 11(3):17-24.
22. Sudhakara Reddy AV, Damodar Reddy M, Krishna Reddy YV. Feeder Reconfiguration of Distribution Systems for Loss Reduction and Emissions Reduction using MVO Algorithm, Majlesi Journal of Electrical Engineering. 2018; 12(2):1-8.
23. Kalyani S, Sudhakara Reddy AV, Vara Prasad N. Optimal Placement of Capacitors in Distribution Systems for Emission Reduction using Ant Lion Optimization Algorithm, International Journal of Current Advanced Research. 2018; 7(11):16339-16343.
24. Sudip Sardar, Mr. Kamalakar P, Mr. Sudhakara Reddy AV, Dr. Ezhil Vignesh K. Car Parking Monitoring System using LabVIEW, Journal of Research in Science, Technology, Engineering and Management (JoRSTEM). 2019; 5(1):66-72.
25. Ram Shankar Singh, Naveen Venkat V, Mr. Sudhakara Reddy AV, Dr. D. Raja Reddy. IOT Home Automation via Google Assistance, Journal of Research in Science, Technology, Engineering and Management (JoRSTEM). 2019; 5(1):44-53.
26. Priyanka G, Prudhvi Raj M, Mr. Ramesh D, Mr. Sudhakara Reddy AV. Human Safety Device using GSM and GPS Module, Journal of Research in Science, Technology, Engineering and Management (JoRSTEM). 2019; 5(1):83-88.
27. Manogna Reddy V, Dr. Raja Reddy D, Mrs. Sudha Reddy Y, Mr. Sudhakara Reddy AV. Effective Load Sharing of Distribution Transformer using GSM, Journal of Research in Science, Technology, Engineering and Management (JoRSTEM). 2019; 5(1):73-77.
28. Krishna Reddy YV, Damodar Reddy M, Sudhakara Reddy AV. Flower Pollination Algorithm for Solving Economic Dispatch with Prohibited Operating Zones and Ramp Rate Limit Constraints, Journal of Emerging Technologies and Innovative Research (JETIR). 2018; 5(10):498-505.
29. Sudhakara Reddy AV, Rajeswaran N, Raja Reddy D. Application of modified ALO to economic load dispatch for coal fired stations,

International Journal of Recent Technology and Engineering (IJRTE). 2019; 8(2):2147-2152.

30. Jhansi Reddy, Nikitha Reddy, Raja Reddy D, Dr. Sudhakara Reddy AV. Smart Traffic Control System using Sensors, International Journal of Research and Advanced Development (IJRAD). 2019; 3(3):14-16. ISSN: 2581-4451.
31. Krishna Reddy YV, Damodar Reddy M, Sudhakara Reddy AV. Flower Pollination Algorithm to Solve Dynamic Economic Loading of Units with Practical Constraints, International Journal of Recent Technology and Engineering (IJRTE). 2019; (3):535-542.
32. Sabarinath G, Gowri Manohar T, Sudhakara Reddy AV. Voltage Control and Power Loss Reduction in Distribution Networks using Distributed Generation, International Journal of Innovative Technology and Exploring Engineering (IJITEE). 2019; 8(12):2863-2867.
33. Praveen Kumar Reddy Y, Vara Prasad N, Sudhakara Reddy AV. A Power Sensor Tag with Interference Reduction for Electricity Monitoring of Two-Wire Household Appliances, Journal of Research in Science, Technology, Engineering and Management (JoRSTEM). 2020; 6(1):31-35.
34. Bhargava Reddy B, Nagarjuna P, Sudhakara Reddy AV. Traffic Signal Control Using Lab View, Journal of Research in Science, Technology, Engineering and Management (JoRSTEM). 2020; 6(1):1-4.
35. Sudhakara Reddy AV, Laxmidevi Ramanaiah M, Krishna Reddy YV, Navya B, Hari Krishna K, Mahender A. Feeder Protection from Over Load Situations through IoT, International Journal of Future Generation Communication and Networking. 2020; 13(3):3699-3707. ISSN: 2233-7857.
36. D. Raja Reddy, Anitha Reddy K, Narendra Kumar Ch, Siva Sai Rama Krishna R, Sudhakara Reddy AV, Rajesh Reddy. Duvvuru Design of Transformer Less UPFC based on Multilevel Inverter, International Journal of Electrical Engineering and Technology (IJEET), 2020, 11(4).
37. Ch. Narendra Kumar, Rajesh Reddy D, Raja Reddy D, Sudhakara Reddy AV, Manoz Kumar Reddy K. Histogram Pattern and Kalman Filter Approach Based Real Time Object Recognition and Tracking System Journal of Critical Reviews. 2020; 7(6):1282-1289.
38. Sudhakara Reddy AV, Md. Imran Ahmed, Ch. Rami Reddy, Ch. Narendra Kumar. Power Quality Improvement in Integrated System

using Inductive UPQC, International Journal of Renewable Energy Research (IJRER). 2021; 11(2):566-576.

39. Kubo S, Nakajima H, Kasahara S, Higashi S, Masaki T, Abe H *et al*. A demonstration study on a closed cycle hydrogen production by the thermochemical water splitting iodine-sulphur process. Nuclear Engineering and Design. 2004; 233:347-354.

Chapter - 6
Scheduling of Hydro-Coal Fired Power Plants

Authors

Dr. A. Pulla Reddy
Associate Professor, ECE, Chadalawada Ramanamma Engineering College, Tirupati, Andhra Pradesh, India

Dr. M. Lakshmikantha Reddy
Associate Professor, EEE, Aditya College of Engineering, Madanapalle, Andhra Pradesh, India

Ch. Narendra Kumar
Associate Professor, EEE, Malla Reddy Engineering College, Secunderabad, Telangana, India

Dr. Y.V. Krishna Reddy
Assistant Professor, Department of EEE, S.V. College of Engineering, JNTUA, Tirupati, Andhra Pradesh, India

Chapter - 6

Scheduling of Hydro-Coal Fired Power Plants

Dr. A. Pulla Reddy, Dr. M. Lakshmikantha Reddy, Ch. Narendra Kumar and Dr. Y.V. Krishna Reddy

Abstract

This chapter presents a method for scheduling hydrothermal power systems based on the Lagrangian relaxation technique. By using Lagrange multipliers to relax system-wide demand and reserve requirements, the problem is decomposed and converted into a two-level optimization problem. Given the sets of Lagrange multipliers, a hydro unit sub-problem is solved by a merit order allocation method, and a thermal unit sub-problem is solved by using dynamic programming without discrediting generation levels. A sub-gradient algorithm is used to update the Lagrange multipliers. Numerical results based on Northeast Utilities data show that this algorithm is efficient, and near-optimal solutions are obtained. Comparing with our previous work where thermal units were scheduled by using the Lagrangian relaxation technique and hydro units by heuristics, the new Co-ordinated hydro and thermal scheduling generates lower total costs.

Keywords: hydro, thermal power plant, demand, load, short time scheduling

1.1 Introduction

No state or country endowed with plenty of water sources or abundant coal and nuclear fuel. For minimum environmental pollution, thermal generation should be minimum. Hence, a mix of hydro and thermal power generation is necessary.

The states that have a large hydro potential can supply excess hydro-power during periods of high-water run-off to other states and can receive thermal power during low water run-off from other states. The states, which have a low hydro-potential and large coal reserves, can use the small amount of hydro-power for meeting peak load requirements. This makes the thermal stations to operate at high load factors and to have reduced installed capacity with the result economy. In states, which have adequate hydro as well as thermal power generation capacities, power co-ordination to obtain most economical operating state is essential.

1.2 Hydro-thermal co-ordination

Initially, there were mostly thermal power plants to generate electrical power. There is a need for the development of hydro-power plants due to the following reasons.

i) Due to the increment of power in the load demand from all sides such as industrial, agricultural, commercial and domestic.

ii) Due to the high cost of fuel (Coal).

iii) Due to the limited range of fuel (Coal).

The hydro plants can be started easily and can be assigned a load in very short time. However, in the case of thermal plants, it requires several to make boilers, super heater and turbine system ready to supply the load. For this reason, the hydro-plants can handle fast changing loads effectively. The thermal plants in contrast are slow in response. Hence due to this, thermal plants suitable to operate as *base load plants* and hydro-plants to operate as *peak load plants*.

Type of plant	Time for synchronization	Operate
Gas Plant	2 Minutes	Peak load plants
Steam plant	8-10 Hr	Base load plants
Hydro-power	5-10 Minutes	Peak load plants

Maximum advantage of cheap hydro power should be taken so that the coal reserves can be conserved and environmental pollution can be minimized. The whole or part of the base load can be supplied by the run-off river hydro-plants and the remaining load is then met by a proper mix of reservoir-type hydro plants and thermal plants.

This hydro-thermal co-ordination is classified into

i) Short-term co-ordination.

ii) Long-term co-ordination.

The operating cost of thermal plants is very high and at the same time, its capital cost is low when compared with a hydro-electric plant. The operating cost of hydro-electric plants is low and its capital cost is high such that it has become economical as well as convenient to run both the plants in the same grid.

Type of Plant	Operating Cost	Capital Cost
Coal-fired plant	High	Low
Hydro-power	Low	High

In the case of thermal plants, the optimal scheduling problem can be completely solved at any instant without referring to the operation at other times. It is a *static optimization problem.*

The operation of a system having both hydro and thermal plants is more complex as hydro-plants have a negligible operating cost but are required to run under the constraint of availability of water for hydro-generation during a given period of time. This problem is '*dynamic optimization problem'*, where the time factor is to be considered.

Consider a simple hydro-thermal system, shown in Fig. 2.3., which consists of one hydro and one thermal plant supplying power to the load connected at the center in between the plants and is referred to as fundamental system.

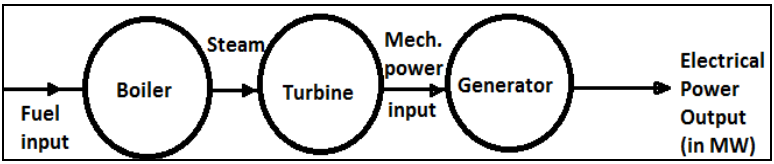

Fig 2.1: Fundamental thermal generating system

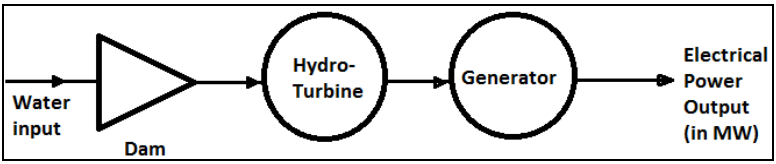

Fig 2.2: Fundamental hydro-system

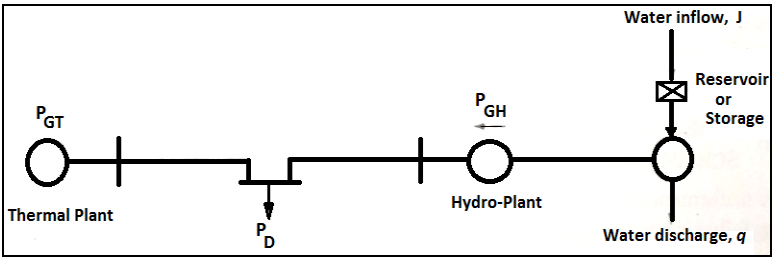

Fig 2.3: Fundamental hydro-thermal system

To solve the optimization problem in this system, consider the real power generations of two plants $P_{G,Thermal}$ *and* $P_{G,Hydel}$ as control variables. The transmission loss is expressed in terms of the B coefficients as

$$P_L = \sum_{i=1}^{n}\sum_{j=1}^{n} P_{Gi} B_{ij} P_{Gj}$$

1.3 Scheduling of hydro units in a hydro-thermal scheduling

i) In case of hydro-units without thermal units in the system, the problem is simple. The economic scheduling consists of scheduling water release to satisfy the hydraulic constraints and to satisfy the electrical demand.

ii) Where hydro-thermal scheduling systems are predominantly hydro scheduling may be done by scheduling the system to produce minimum cost for the thermal systems.

iii) In systems, where, there is a close balance between hydro and thermal generation and in systems where the hydro capacity is only a fraction of the total capacity, it is generally desired schedule generation such that thermal generating costs are minimized.

1.3.1 Long-range hydro-scheduling

The long-range hydro-scheduling problem involves the long-range forecasting of water availability and the scheduling of reservoir water releases (i.e., “drawdown”) for an interval of time that depends on the reservoir capacities. Typical long-range scheduling goes anywhere from 1 wk to 1 yr or several years. For hydro schemes with a capacity of impounding water over several seasons, the long-range problem involves meteorological and statistical analyses.

1.3.2 Short-range hydro-scheduling

Short-range hydro-scheduling (1 day to I wk) involves the hour-by-hour scheduling of all generation on a system to achieve minimum production cost for the given time period. In such a scheduling problem, the load, hydraulic inflows, and unit availabilities are assumed known. A set of starting conditions (e.g., reservoir levels) is given, and the optimal hourly schedule that minimizes a desired objective, while meeting hydraulic steam, and electric system constraints, is sought.

Hydrothermal systems where the hydroelectric system is by far the largest component may be scheduled by economically scheduling the system to produce the minimum cost for the thermal system. The schedules are usually developed to minimize thermal generation production costs, recognizing all the diverse hydraulic constraints that may exist.

1.4 Solution of short-term hydro-thermal scheduling problems-Kirchmayer's method

In this method, the co-ordination equations are derived in terms of penalty factors of both plants for obtaining the optimum scheduling of a

hydro-thermal system and hence it is also known as the of *penalty factor method* solution of short-term Hydro-Thermal Scheduling Problems.

Let

$P_{GTi} \rightarrow$ *be the power generation of* i^{th} *thermal plant in MW*

$P_{GHj} \rightarrow$ *be the power generation of* j^{th} *hydro-plant in MW*

$\frac{dC_i}{dP_{GTi}} \rightarrow$ *be the incremental fuel cost* i^{th} *thermal plant in MW*

$w_j \rightarrow$ *be the quantity of water used for power generation at* j^{th} *hydro-plant in* m^3/s

$\frac{dw_j}{dP_{GHj}} \rightarrow$ *be the incremental water rate of* j^{th} *hydro-plant in* $m^3/s/MW$

$\frac{dP_L}{dP_{GTi}} \rightarrow$ *be the incremental transmission loss of* i^{th} *thermal plant*

$\frac{dP_L}{dP_{GHj}} \rightarrow$ *be the incremental transmission loss of* j^{th} *hydro-plant*

$\lambda \rightarrow$ *be the Lagrangian multiplier*

$\gamma_j \rightarrow$ *be the constant which converts the incremental water rate of hydel plant-j into an incremental cost*

$n \rightarrow$ *be the total number of plants*

$\alpha \rightarrow$ *be the number of thermal plants*

$n\text{-}\alpha \rightarrow$ *be the number of hydro-plants and*

$T \rightarrow$ *be the time interval during which the plant operation is considered*

Here, the objective is to find the generation of individual plants, both thermal as well as hydel that the generation cost (cost of fuel in thermal) is optimum and at the same time total demand (P_D) and losses (P_L) are continuously met.

As it is a short-range Problem, there will not be any appreciable change in the level of water in the reservoirs during the interval (i.e. the effects of rainfall and evaporation are neglected) and hence the head of water in the reservoir will be assumed to be constant.

Let K_j be the specified quantity of water, which must be utilized within the interval T at each hydro-station *j*.

Problem formulation

The objective function is to minimize the cost of generation:

$$\text{i.e., } min \sum_{i=1}^{\alpha} \int_{0}^{T} C_i \, dt \qquad \ldots (1)$$

Subjected to the equality constraints

$$\sum_{i=1}^{\alpha} P_{GTi} + \sum_{j=\alpha+1}^{n} P_{GHj} = P_D + P_L \qquad \ldots (2)$$

$$\text{And } \int_{0}^{t} w_j \, dt = K_j \qquad \text{.....(3) } for\ j=\alpha+1,.....n$$

Where, w_j is the turbine discharge in the j^{th} plant m^3/s and

K_j the amount of water in m^3 utilized during the time period T in the j^{th} hydro plant.

The coefficient γ must be selected so as to use the specified amount of water during the operating period.

Now the objective function becomes

$$min\ C = \sum_{i=1}^{\alpha} \int_{0}^{T} C_i \, dt + \sum_{j=\alpha+1}^{n} \gamma_j K_j \qquad \ldots (4)$$

sub eq.(3) into eq.(4) then we get

$$min\ C = \sum_{i=1}^{\alpha} \int_{0}^{T} C_i \, dt + \sum_{j=\alpha+1}^{n} \gamma_j \int_{0}^{t} w_j \, dt \qquad \ldots (5)$$

For a particular load demand P_D eq.(2) becomes

$$\sum_{i=1}^{\alpha} \Delta P_{GTi} + \sum_{j=\alpha+1}^{n} \Delta P_{GHj} - \sum_{i=1}^{\alpha} \frac{\partial P_L}{\partial P_{GTi}} \Delta P_{GTi} - \sum_{j=\alpha+1}^{n} \frac{\partial P_L}{\partial P_{GHj}} \Delta P_{GHj} = 0$$

$$\sum_{i=1}^{\alpha} \left(1 - \frac{\partial P_L}{\partial P_{GTi}}\right) \Delta P_{GTi} + \sum_{j=\alpha+1}^{n} \left(1 - \frac{\partial P_L}{\partial P_{GHj}}\right) \Delta P_{GHj} = 0 \qquad \ldots (6)$$

For a particular hydro-plant x, The eq.(6) can be written as

$$\sum_{i=1}^{\alpha}\left(1-\frac{\partial P_L}{\partial P_{GTi}}\right)\Delta P_{GTi}+\left(1-\frac{\partial P_L}{\partial P_{GHx}}\right)\Delta P_{GHx}+\sum_{\substack{j=\alpha+1\\ j\neq x}}^{n}\left(1-\frac{\partial P_L}{\partial P_{GHj}}\right)\Delta P_{GHj}=0 \quad \ldots (7)$$

$$\left(1-\frac{\partial P_L}{\partial P_{GHx}}\right)\Delta P_{GHx}=-\sum_{i=1}^{\alpha}\left(1-\frac{\partial P_L}{\partial P_{GTi}}\right)\Delta P_{GTi}-\sum_{\substack{j=\alpha+1\\ j\neq x}}^{n}\left(1-\frac{\partial P_L}{\partial P_{GHj}}\right)\Delta P_{GHj}$$

From eq.(5), the condition for minimization is

$$\Delta\left[C=\sum_{i=1}^{\alpha}\int_0^T C_i\,dt+\sum_{j=\alpha+1}^{n}\gamma_j\int_0^t w_j\,dt\right]=0$$

$$\sum_{i=1}^{\alpha}\frac{dC_i}{dP_{GTi}}.\Delta P_{GTi}+\sum_{j=\alpha+1}^{n}\gamma_j\frac{dw_j}{dP_{GHj}}.\Delta P_{GHj}=0$$

For hydro-plant x,

$$\sum_{i=1}^{\alpha}\frac{dC_i}{dP_{GTi}}.\Delta P_{GTi}+\gamma_x\frac{dw_x}{dP_{GHx}}.\Delta P_{GHj}+\sum_{\substack{j=\alpha+1\\ j\neq x}}^{n}\gamma_j\frac{dw_j}{dP_{GHj}}\Delta P_{GHj}=0$$

$$\gamma_x\frac{dw_x}{dP_{GHx}}.\Delta P_{GHj}=-\sum_{i=1}^{\alpha}\frac{dC_i}{dP_{GTi}}.\Delta P_{GTi}-\sum_{\substack{j=\alpha+1\\ j\neq x}}^{n}\gamma_j\frac{dw_j}{dP_{GHj}}\Delta P_{GHj}$$

Multiplying the above equation by $\left(1-\frac{\partial P_L}{\partial P_{GHx}}\right)$

$$\gamma_x\left(1-\frac{\partial P_L}{\partial P_{GHx}}\right)\frac{dw_x}{dP_{GHx}}.\Delta P_{GHj}=\left(1-\frac{\partial P_L}{\partial P_{GHx}}\right)\left[-\sum_{i=1}^{\alpha}\frac{dC_i}{dP_{GTi}}.\Delta P_{GTi}-\sum_{\substack{j=\alpha+1\\ j\neq x}}^{n}\gamma_j\frac{dw_j}{dP_{GHj}}\Delta P_{GHj}\right] \quad \ldots (8)$$

Substituting $\left(1-\frac{\partial P_L}{\partial P_{GHx}}\right)\Delta P_{GHj}$ from eq.(7) into eq.(8) then we get,

$$\gamma_x\frac{dw_x}{dP_{GHx}}.\left[-\sum_{i=1}^{\alpha}\left(1-\frac{\partial P_L}{\partial P_{GTi}}\right)\Delta P_{GTi}-\sum_{\substack{j=\alpha+1\\ j\neq x}}^{n}\left(1-\frac{\partial P_L}{\partial P_{GHj}}\right)\Delta P_{GHj}\right]=\left(1-\frac{\partial P_L}{\partial P_{GHx}}\right)\left[-\sum_{i=1}^{\alpha}\frac{dC_i}{dP_{GTi}}.\Delta P_{GTi}-\sum_{\substack{j=\alpha+1\\ j\neq x}}^{n}\gamma_j\frac{dw_j}{dP_{GHj}}\Delta P_{GHj}\right]$$

Rewriting the above equation as

$$\sum_{i=1}^{\alpha}\left[\frac{dC_i}{dP_{GTi}}\left(1-\frac{\partial P_L}{\partial P_{GHx}}\right)-\gamma_x\frac{dw_x}{dP_{GHx}}.\left(1-\frac{\partial P_L}{\partial P_{GTi}}\right)\right]\Delta P_{GTi}+\sum_{\substack{j=\alpha+1\\ j\neq x}}^{n}\left[\gamma_j\frac{dw_j}{dP_{GHj}}.\left(1-\frac{\partial P_L}{\partial P_{GHx}}\right)-\gamma_x\frac{dw_x}{dP_{GHx}}.\left(1-\frac{\partial P_L}{\partial P_{GHj}}\right)\right]\Delta P_{GHj}=0 \quad \ldots (9)$$

$\therefore \Delta P_{GTi}\neq 0$ *and* $\Delta P_{GHj}\neq 0$, *Eq.(9) becomes*

$$\left[\frac{dC_i}{dP_{GTi}}\left(1-\frac{\partial P_L}{\partial P_{GHx}}\right)-\gamma_x\ \frac{dw_x}{dP_{GHx}}.\left(1-\frac{\partial P_L}{\partial P_{GTi}}\right)\right]=0 \qquad \ldots (10)$$

$$and\left[\gamma_i\ \frac{dw_i}{dP_{GHj}}.\left(1-\frac{\partial P_L}{\partial P_{GHx}}\right)-\gamma_x\ \frac{dw_x}{dP_{GHx}}.\left(1-\frac{\partial P_L}{\partial P_{GHj}}\right)\right]=0 \qquad \ldots (11)$$

Equation (10) can be written as

$$(10)\Rightarrow\ \frac{dC_i}{dP_{GTi}}\left(1-\frac{\partial P_L}{\partial P_{GHx}}\right)-\gamma_x\ \frac{dw_x}{dP_{GHx}}.\left(1-\frac{\partial P_L}{\partial P_{GTi}}\right)=0$$

$$\Rightarrow\ \frac{dC_i}{dP_{GTi}}\left(1-\frac{\partial P_L}{\partial P_{GHx}}\right)=\gamma_x\ \frac{dw_x}{dP_{GHx}}.\left(1-\frac{\partial P_L}{\partial P_{GTi}}\right)$$

$$\frac{dC_i}{dP_{GTi}}\frac{1}{\left(1-\frac{\partial P_L}{\partial P_{GTi}}\right)}=\gamma_x\ \frac{dw_x}{dP_{GHx}}.\frac{1}{\left(1-\frac{\partial P_L}{\partial P_{GHx}}\right)} \qquad \ldots (12)$$

Equation (11) can be written as

$$(11)\Rightarrow\gamma_j\ \frac{dw_j}{dP_{GHj}}.\left(1-\frac{\partial P_L}{\partial P_{GHx}}\right)-\gamma_x\ \frac{dw_x}{dP_{GHx}}.\left(1-\frac{\partial P_L}{\partial P_{GHj}}\right)=0$$

$$\Rightarrow\gamma_j\ \frac{dw_j}{dP_{GHj}}.\left(1-\frac{\partial P_L}{\partial P_{GHx}}\right)=\gamma_x\ \frac{dw_x}{dP_{GHx}}.\left(1-\frac{\partial P_L}{\partial P_{GHj}}\right)$$

$$\gamma_j\ \frac{dw_j}{dP_{GHj}}.\frac{1}{\left(1-\frac{\partial P_L}{\partial P_{GHj}}\right)}=\gamma_x\ \frac{dw_x}{dP_{GHx}}.\frac{1}{\left(1-\frac{\partial P_L}{\partial P_{GHx}}\right)} \qquad \ldots (13)$$

From Equations (12) & (13) we have

$$\frac{dC_i}{dP_{GTi}}\ \frac{1}{\left(1-\frac{\partial P_L}{\partial P_{GTi}}\right)}\ =\ \gamma_x\ \frac{dw_x}{dP_{GHx}}.\ \frac{1}{\left(1-\frac{\partial P_L}{\partial P_{GHx}}\right)}=\lambda \qquad \ldots (14)$$

$$\frac{dC_i}{dP_{GTi}}\frac{1}{\left(1-\frac{\partial P_L}{\partial P_{GTi}}\right)}=(IC)_i\ .\ L_i\ =\ \lambda \qquad for\ \ i=1,2,3.....\alpha$$

$$\gamma_j\ \frac{dw_j}{dP_{GHj}}.\ \frac{1}{\left(1-\frac{\partial P_L}{\partial P_{GHj}}\right)}\ =\ \gamma_x\ \frac{dw_x}{dP_{GHx}}.\ \frac{1}{\left(1-\frac{\partial P_L}{\partial P_{GHx}}\right)} \qquad \ldots (15)$$

$$\gamma_j\ \frac{dw_j}{dP_{GHj}}.\ \frac{1}{\left(1-\frac{\partial P_L}{\partial P_{GHj}}\right)}\ =\ \gamma_j\ (I_W)_j\ L_j\ =\lambda \qquad for\ \ j=\alpha+1,\ \alpha+2,\ \alpha+3,\ .....N$$

Where,

$(IC)_i$ is the incremental cost of the i^{th} thermal plant.

$(I_W)_j$ is the incremental water rate of the j^{th} hydro-plant.

Equations (14) & (15) may be expressed approximately as

$$\frac{dC_i}{dP_{GTi}}\left(1+\frac{\partial P_L}{\partial P_{GTi}}\right) = \lambda \qquad for\ i=1,2,3.....\alpha \qquad \ldots (16)$$

$$\gamma_j \ \frac{dw_j}{dP_{GHj}}.\left(1+\frac{\partial P_L}{\partial P_{GHj}}\right) = \lambda \qquad for\ j=\alpha+1,\ \alpha+2,\ \alpha+3,\ .....N \qquad \ldots (17)$$

where $\left(1+\frac{\partial P_L}{\partial P_{GTi}}\right)$ *and* $\left(1-\frac{\partial P_L}{\partial P_{GHj}}\right)$ *are the approximate penalty factors of the* i^{th} *thermal plant and* j^{th} *hydro-plant respectively.*

The above Eq.(14) and Eq.(15) are the co-ordinate equations, which are used to obtain the optimal scheduling of the hydro-thermal system when considering the transmission losses.

In the above equations, the transmission loss P_L is expressed as

$$P_L = \sum_{i=1}^{\alpha}\sum_{k=1}^{\alpha} P_{GTi}\, B_{ik}\, P_{GTk} + \sum_{g=\alpha+1}^{n}\sum_{j=\alpha+1}^{n} P_{GHj}\, B_{gj}\, P_{GHj} + 2\sum_{i=1}^{\alpha}\sum_{j=\alpha+1}^{n} P_{GTi}\, B_{ij}\, P_{GHj} \ldots (18)$$

The power generation of a hydro-plant P_{GHj} is directly proportional to its head and discharge rate W_j. When neglecting the transmission losses, the co-ordination equations become

$$\frac{dC_i}{dP_{GTi}} = \lambda \ and\ \gamma_j \ \frac{dw_j}{dP_{GHj}} = \lambda$$

1.5 Conclusion

Power exchange with other utilities is not included here. Since this is the optimization problem, any model simplification results in worsening of results. Instead of taking billing rules of authors should have modeled the river basin precisely. The hydro sub-problem, as it is formulated in the chapter, is a linear programming problem with upper and lower constraints and nonlinear production characteristics of hydro power plants are not taken into account. As it is formulated, the sub problem solution will have results on upper and lower bounds and oscillations in the process solution may appear, as it was mentioned in the paper.

References

1. De Boer R. Technologies and Prospects for Photochemical Conversion and Storage of Solar Energy: A survey of the state-of-threat, ed., ECN-C--01-029, 2001, 7-9.
2. Baird C. Environmental Chemistry, 2nd ed., Freeman WH and Company, NY, 1999, 251-251.
3. www.google.com
4. Chopra KL. Thin Film Phenomena, (McGraw Hill, New York), 1969.
5. Brown MP, Austin K. Appl. Phys. Letters. 2004; 85:2503-2504.
6. Improvement of reactor efficiency by steam entrainment. International Journal of Hydrogen Energy, 25, 739-745.
7. Sudhakara Reddy AV, Ramasekhara Reddy M, Vijaya Kumar M. Stability Improvement During Damping of Low Frequency Oscillations with Fuzzy Logic Controller, International Journal of Engineering Research and Applications (IJERA). 2012; 2(5):1560-1565.
8. Bhargava Reddy B, Sivakrishna D, Sudhakara Reddy AV. Modelling and Analysis of Wind Power Generation Using PID Controller, International Journal for Scientific Research & Development (IJSRD). 2013; 1(9):2045-2049.
9. Prasad P, Bhargava Reddy B, Sudhakara Reddy AV. Power Loss Minimization in Distribution System using Network Reconfiguration with Particle Swarm Optimization, International Journal of Engineering Science & Advanced Technology (IJESAT). 2015; 5(3):171-178.
10. Surekha K, Sudhakara Reddy AV. A New Control Topology for Smart Power Grids using Bi-directional Synchronous VSC, International Journal of Informative & Futuristic Research. 2015; 2(10):3695-3704.
11. Sudhakara Reddy AV, Damodar Reddy M, Vinoda N. Optimal Placement of Dynamic Voltage Restorer in Distribution Systems for Voltage Improvement Using Particle Swarm Optimization, International Journal of Engineering Research and Applications (IJERA). 2017; 7(3):29-33. ISSN: 2248-9622.
12. Sudhakara Reddy AV, Damodar Reddy M. Optimization of Distribution Network Reconfiguration Using Dragonfly Algorithm, Journal of Electrical Engineering. 2017; 16(4-30):273-282. ISSN:1582-1594.

13. Bharathi S, Sudhakara Reddy AV, Damodar Reddy M. Optimal Placement of UPFC and SVC using Moth-Flame Optimization Algorithm, International Journal of Soft Computing and Artificial Intelligence. 2017; 5(1):41-45.
14. Sudhakara Reddy AV, Damodar Reddy M. Optimal Capacitor allocation for the reconfigured Network using Ant Lion Optimization algorithm, International Journal of Applied Engineering Research (IJAER). 2017; 12(12):3084-3089.
15. Sudhakara Reddy AV, Damodar Reddy M. Network Reconfiguration of Distribution System for maximum loss reduction using Sine Cosine Algorithm, International Journal of Engineering Research and Applications (IJERA). 2017; 7(10):34-39.
16. Sudhakara Reddy AV, Damodar Reddy M, Satish Kumar Reddy M. Network Reconfiguration of Distribution Systems for Loss Reduction using GWO algorithm, International Journal of Electrical and Computer Engineering (IJECE). 2017; 7(6):3226-3234.
17. Sudhakara Reddy AV, Damodar Reddy M. Distribution Network Reconfiguration for Maximum Loss Reduction using Moth Flame Optimization, International Journal of Emerging Technologies in Engineering Research (IJETER). 2018; 6(1):86-90.
18. Sudhakara Reddy AV, Dr. Damodar Reddy M. Application of Whale Optimization Algorithm for Distribution Feeder Reconfiguration, i-manager's Journal on Electrical Engineering. 2018; 11(3):17-24.
19. Sudhakara Reddy AV, Damodar Reddy M, Krishna Reddy YV. Feeder Reconfiguration of Distribution Systems for Loss Reduction and Emissions Reduction using MVO Algorithm, Majlesi Journal of Electrical Engineering. 2018; 12(2):1-8.
20. Kalyani S, Sudhakara Reddy AV, Vara Prasad N. Optimal Placement of Capacitors in Distribution Systems for Emission Reduction Using Ant Lion Optimization Algorithm, International Journal of Current Advanced Research. 2018; 7(11):16339-16343.
21. Sudip Sardar, Mr. Kamalakar P, Mr. Sudhakara Reddy AV, Dr. Ezhil Vignesh K. Car Parking Monitoring System Using LabVIEW, Journal of Research in Science, Technology, Engineering and Management (JoRSTEM). 2019; 5(1):66-72.
22. Sudhakara Reddy AV, Praveen Kumar Reddy Y, Bhargava Reddy B, Krishna Reddy YV. Application of ALO to Economic Load Dispatch

Without Network Losses for Different Conditions, 2nd IEEE International Conference on Power Electronics, Intelligent Control and Energy Systems (ICPEICES), New Delhi, India, 2018, 244-248.

23. Ram Shankar Singh, Naveen Venkat V, Mr. Sudhakara Reddy AV, Dr. Raja Reddy D. IOT Home Automation via Google Assistance, Journal of Research in Science, Technology, Engineering and Management (JoRSTEM). 2019; 5(1):44-53.
24. Priyanka G, Prudhvi Raj M, Mr. Ramesh D, Mr. Sudhakara Reddy AV. Human Safety Device using GSM and GPS Module, Journal of Research in Science, Technology, Engineering and Management (JoRSTEM). 2019; 5(1):83-88.
25. Manogna Reddy V, Dr. Raja Reddy D, Mrs. Y Sudha Reddy, Mr. Sudhakara Reddy AV. Effective Load Sharing of Distribution Transformer using GSM", Journal of Research in Science, Technology, Engineering and Management (JoRSTEM). 2019; 5(1):73-77.
26. Krishna Reddy YV, Damodar Reddy M, Sudhakara Reddy AV. Flower Pollination Algorithm for Solving Economic Dispatch with Prohibited Operating Zones and Ramp Rate Limit Constraints, Journal of Emerging Technologies and Innovative Research (JETIR). 2018; 5(10):498-505.
27. Sudhakara Reddy AV, Rajeswaran N, Raja Reddy D. Application of modified ALO to economic load dispatch for coal fired stations, International Journal of Recent Technology and Engineering (IJRTE). 2019; 8(2):2147-2152.
28. Jhansi Reddy, Nikitha Reddy, Raja Reddy D, Dr. Sudhakara Reddy AV. Smart Traffic Control System using Sensors, International Journal of Research and Advanced Development (IJRAD). 2019; 3(3):14-16. ISSN: 2581-4451.
29. Krishna Reddy YV, Damodar Reddy M, Sudhakara Reddy AV. Flower Pollination Algorithm to Solve Dynamic Economic Loading of Units with Practical Constraints, International Journal of Recent Technology and Engineering (IJRTE). 2019; 8(3):535-542.
30. Sudhakara Reddy AV, Prof. M Damodar Reddy. Optimization of network reconfiguration by using particle swarm optimization, IEEE First International Conference on Power Electronics, Intelligent Control and Energy Systems (IEEE ICPEICES), Delhi Technological University (DTU), New Delhi, India, 2016, 1-6.

31. Sabarinath G, Gowri Manohar T, Sudhakara Reddy AV. Voltage Control and Power Loss Reduction in Distribution Networks using Distributed Generation, International Journal of Innovative Technology and Exploring Engineering (IJITEE). 2019; 8(12):2863-2867.
32. Praveen Kumar Reddy Y, Vara Prasad N, Sudhakara Reddy AV. A Power Sensor Tag with Interference Reduction for Electricity Monitoring of Two-Wire Household Appliances, Journal of Research in Science, Technology, Engineering and Management (JoRSTEM). 2020; 6(1):31-35.
33. Bhargava Reddy B, Nagarjuna P, Sudhakara Reddy AV. Traffic Signal Control Using Lab View, Journal of Research in Science, Technology, Engineering and Management (JoRSTEM). 2020; 6(1):1-4.
34. Sudhakara Reddy AV, Laxmidevi Ramanaiah M, Krishna Reddy YV, Navya B, Hari Krishna K, Mahender A. Feeder Protection from Over Load Situations through IoT, International Journal of Future Generation Communication and Networking. 2020; 13(3):3699-3707. ISSN: 2233-7857.
35. Raja Reddy D, Anitha Reddy K, Narendra Kumar Ch, Siva Sai Rama Krishna R, Sudhakara Reddy AV, Rajesh Reddy. Duvvuru Design of Transformer Less UPFC based on Multilevel Inverter, International Journal of Electrical Engineering and Technology (IJEET), 2020, 11(4).
36. Ch. Narendra Kumar, Rajesh Reddy D, Raja Reddy D, Sudhakara Reddy AV, Manoz Kumar Reddy K. Histogram Pattern and Kalman Filter Approach Based Real Time Object Recognition and Tracking System Journal of Critical Reviews. 2020; 7(6):1282-1289.
37. Sudhakara Reddy AV, Md. Imran Ahmed, Ch. Rami Reddy, Ch. Narendra Kumar. Power Quality Improvement in Integrated System using Inductive UPQC, International Journal of Renewable Energy Research (IJRER), 2021.